Technische Universität München
Fakultät für Medizin

The role of TGFβ1 in tumour initiation and progression of pancreatic cancer

Evelyn Natalie Krohmer

Vollständiger Abdruck der von der Fakultät für Medizin der Technischen Universität München zur Erlangung einer

Doktorin der Medizin (Dr. med)

genehmigten Dissertation.

Vorsitz: Prof. Dr. Marcus Makowski

Prüfer*innen der Dissertation:

1. Prof. Dr. Dieter Saur
2. Prof. Dr. Günter Schneider

Die Dissertation wurde am 28.06.2022 bei der Technischen Universität München eingereicht und durch die Fakultät für Medizin am 21.03.2023 angenommen.

Table of contents

List of figures

List of tables

List of abbreviations

°C	degree Celsius
%	Percent
Bcl-2	b-cell lymphoma 2
BMP	bone morphogenetic protein
bp	base pair
BW	body weight
CAF	cancer-associated fibroblasts
CDK	cyclin-dependent kinase
CDKN2A	cyclin-dependent kinase inhibitor 2A
cDNA	complementary deoxyribonucleic acid
CIS	carcinoma in situ
Ck19	cytokeratin-19
cm	centimetre
cm^2	square centimetre
Co-SMAD	common SMAD
CRB	crumbs complexes
DMEM	Dulbecco´s modified eagle medium
DMSO	dimethylsulfoxide
DNA	deoxyribonucleic acid
dNTP	deoxynucleoside triphosphate
DRS	dual-recombinase system
ECM	extracellular matrix
EDTA	ethylenediaminetetraacetic acid
EGFR	epithelial growth factor receptor
EMT	epithelial to mesenchymal transition
EMT-TF	EMT transcription factors
ERK	extracellular signal-related kinase
FCS	fetal calf serum
FOLFIRINOX	fluorouracil, folinic acid, irinotecan, oxaliplatin
FSF	frt-stop-frt
g	gram
GDP	guanosine diphosphate
GEF	guanine nucleotide exchange factor
GEMM	genetically engineered mouse model

GNAS	Guanine nucleotide-binding protein G(s) subunit alpha isoforms short
GTP	guanosine triphosphate
h	hours
H&E	haematoxylin and eosin
hPDAC	human PDAC
i.p.	intraperitoneal
IPMN	intraductal papillary-mucinous neoplasm
I-SMAD	Inhibitory SMAD
kg	kilogram
KRAS	v-Ki-ras2 Kirsten rat sarcoma viral oncogene homolog
L	liter
LAP	latency associated peptide
LLC	large latent complex
LOH	loss of heterozygosity
LSL	loxP-stop-loxP
LTBP	latent TGF-β-binding protein
MAPK	mitogen-activated protein kinase
MCN	mucinous cystic neoplasm
MET	mesenchymal to epithelial transition
mg	milligram
MH	mad homology
min	minute
mL	millilitre
mm	millimetre
mM	millimolar
mPDAC	mouse PDAC
mRNA	messenger ribonucleic acid
mTOR	mammalian target of rapamycin
MTT	3-(4,5-Dimethyl-2-thiazolyl)-2,5-diphenyl-tetrazolium bromide
MUC	mucine
mut	mutated
NADH	nicotinamide adenine dinucleotide
N-Cadherin	neural cadherin
Nm	nanometre
PanIN	pancreatic intraepithelial neoplasia
PAR	partitioning-defective complexes

PBS	phosphate buffered saline
PCR	polymerase chain reaction
PDAC	pancreatic ductal adenocarcinoma
Pdx1	pancreatic and duodenal homeobox 1
PI3K	phosphoinositide 3-kinase
PSC	pancreatic stellate cells
Ptf1a	pancreas transcription factor subunit alpha
R26	Rosa26
Raf	rapidly accelerated fibrosarcoma
RNA	ribonucleic acid
R-SMAD	receptor-regulated SMAD
rpm	rounds per minute
RT	room temperature
s	seconds
SBE	SMAD-binding element
SD	standard deviation
SLC	inactive small latent complex
SMAD	mothers against decapentaplegic homolog
SMURF	SMAD specific E3 ubiquitin protein ligase
TAM	tumour associated macrophages
TGFβ	transforming growth factor beta
TGFβRI	transforming growth factor beta receptor type I
TGFβRII	transforming growth factor beta receptor type II
TME	tumour microenvironment
TP53 / Trp53	transformation related protein 53
Tregs	regulatory T-cells
V	volt
VEGF	vascular endothelial growth factor
WHO	world health organization
WT	wild type
W	watt
µg	microgram
µL	microliter
µm	micrometre
µM	micromolar

1 Abstract

Pancreatic cancer remains, in contrast to other tumour entities, a disease with lacking screening methods, limited therapeutic approaches and a poor prognosis. Underlying genetic alterations in human pancreatic cancer were characterized through genomic sequencing and reliable genetically engineered mouse models with a pancreas-specific activation of *Kras*^{G12D} or *Kras*^{G12V} have been developed, mirroring the most common histological subtype: pancreatic ductal adenocarcinoma (PDAC). However, signalling pathways for tumour cell interaction, metastasis and therapy resistance of PDACs are still poorly understood. Over the years different key signalling pathways were investigated and identified. The transforming growth factor β (TGFβ) pathway came to attention as mutations in pathway members are frequently observed in human PDACs.

Nevertheless, the role of TGFβ signalling in pancreatic cancer initiation and progression is still unclear. Frequent loss-of-function mutations of TGFβ pathway members and cell cycle inhibition support its role as tumour suppressor. However, TGFβ also promotes effects supporting cancer cell growth like creating an immunosuppressive microenvironment, recruiting physiological resources (e.g. blood supply) and facilitating epithelial to mesenchymal transition.

To investigate the effects of TGFβ signalling in context of premalignant and more advanced tumour stages we compared two tissue-specific *Kras*^{G12D}-driven mouse models of PDAC with (1) constitutively active *Tgfβ1* overexpression (PKTo) and (2) tamoxifen-inducible time specific *Tgfβ1* overexpression (FKTo).

We evaluated these mouse models in terms of cancer initiation, progression and metastasis rate in pancreatic tissue *in vivo* using histological analysis at fixed timepoints and at time of sacrifice as well as *in vitro* in cell culture experiments comparing morphology and proliferation.

PKTo mice displayed two different histological phenotypes. 85.2% (n=23) showed cystic papillary lesions and few low-grade pancreatic intraepithelial neoplasia (PanINs). 14.8% (n=4) showed dedifferentiated primary tumours (≥G3) and a 100% metastasis rate with infestations of the liver, lungs or both. In contrast, *Tgfβ1* overexpression without oncogenic *Kras* did not trigger PDAC formation in vivo. Time specific induction of *Tgfβ1* in 3 months old FKTo mice led to dismantling of preformed PanINs, suppression of PDAC development and formation of cystic papillary lesions.

This data suggests that constitutively active *Tgfβ1* has anti-tumorigenic effects on pancreatic tissue in *Kras*^{G12D}-driven mouse models of PDAC. However, few cases develop a tumour suppression escape mechanism and progress into aggressive, metastatic

cancer. Delayed *Tgfβ1* activation *in vivo* suppressed PDAC progression. A combination of *Tgfβ1* overexpression and oncogenic $Kras^{G12D}$ may be an opportunity to generate mouse models mirroring the formation of cystic precursor lesions instead of PanINs.

2 Zusammenfassung

Das Pankreaskarzinom ist heutzutage, trotz allgemein verbesserter Behandlungsmethoden und Gesamtüberleben, immer noch eines der schwierigsten zu behandelnden Tumorentitäten, bei der die 5-Jahres-Überlebensrate über alle Stadien hinweg 11 % beträgt. Gründe hierfür sind vor allem das Fehlen von zuverlässigen Screening-Methoden, die damit einhergehende Erstdiagnose in eher fortgeschrittenen Stadien und somit limitierten therapeutischen Optionen für diese Patienten. Die häufigste histologische Subklasse ist das duktale Adenokarzinom (85-90% aller Fälle) und bisher am meisten erforscht. Während die genetischen Veränderungen im humanen Pankreaskarzinom in den letzten Jahren mit Hilfe neuer Sequenzierungstechnologien eingehend charakterisiert wurden, sind therapeutisch relevante Signalwege die zur Tumoraufrechterhaltung, Metastasierung und Therapieresistenz von PDACs beitragen ebenso unzureichend untersucht und verstanden, wie die Interaktionen der Tumorzellen mit dem Wirt.

Die pankreas-spezifische Expression von onkogenem $Kras^{G12D}$ oder $Kras^{G12V}$ induziert in genetisch definierten Mausmodellen die Entwicklung von invasiven, aggressiven und hochgradig metastasierenden Pankreaskarzinomen, die viele Aspekte der humanen Erkrankung, wie z.B. genetische Instabilität und Metastasierungsverhalten (70% Leber- und Lungenmetastasen) sehr genau rekapitulieren. Sie sind ebenfalls in der Lage die Progression der häufigsten Vorstufenläsionen (PanIN-Läsionen) in der Pankreas zu imitieren und stellen somit ein zuverlässiges Mausmodel dar.

Die Rolle des TGFβ-Signalwegs in den verschiedenen Stadien der Tumorentstehung und -progression ist noch nicht vollständig erforscht. Inaktivierende Mutationen von Botenstoffen des TGFβ-Signalweges und Zellzyklus-Arrest unterstützen die These einer hauptsächlich tumorsuppressiven Funktion. Andererseits fördert TGFβ über andere Mechanismen Tumorzellwachstum, die Entstehung eines immunsuppressiven Milieus, Blutversorgung des Tumors und EMT. Wir gehen davon aus, dass TGFβ einen essentiellen tumorbiologischen Knotenpunkt und eine vielversprechende therapeutische Zielstruktur darstellt.

In dieser Arbeit benutzten wir zwei verschiedene Mausmodelle, eines mit dem neuen dualen Rekombinationssystem (DRS), um dies in vivo und in vitro zu analysieren.

Mausmodelle mit konstitutiv aktiver *Tgfβ1*-Überexpression (=PKTo) entwickelten zwei verschiedene histologische Phänotypen. 85.2% (n=23) zeigten die Bildung von vornehmlich zystischen, papillären Läsionen und wenig ausgeprägte niedriggradige PanIN-Läsionen, während 14.8% (n=4) ein sehr aggressives, entdifferenziertes Karzinom

(≥G3) mit hoher Metastasierungsrate entwickelten. Überexpression von ausschließlich *Tgfβ1* zeigte keinen onkogenen Effekt.

Darüber hinaus führte eine zeit-spezifische, verzögerte Aktivierung von *Tgfβ1* mittels des DRS zu einem Rückgang der durch onkogenes *Kras* ausgelösten, präformierten PanIN Läsionen und der Bildung von zystischen, papillären Läsionen.

Diese Daten könnten darauf hinweisen, dass konstitutiv aktives *Tgfβ1* bei gleichzeitig aktivem *Kras* einen anti-tumorigenen Effekt auf das Pankreasgewebe ausübt, in wenigen Fällen jedoch einen Ausweich-Mechanismus aktiviert und somit zu einem aggressiven, hochmetastatischen Tumor führt. Verzögerte *Tgfβ1*-Überexpression führt unterdessen zu einer Tumor-Regredienz und der Bildung von zystischen Läsionen. Somit könnte die Kombination von *Tgfβ1* und *Kras* zukünftig als neues Mausmodell für die Erforschung von zystischen Vorstuferläsionen und Tumoren genutzt werden.

3 Introduction

3.1 Pancreatic cancer

Cancer is the second-leading cause of death worldwide (Siegel, Miller, Fuchs, & Jemal, 2022). In the United States it is the most common cause of death among elderly people aged 40-79 years (Siegel et al., 2022). Cancer prevalence has increased over the last decades, mainly due to an increase in lifetime expectancy, especially in well-developed countries (Ritchie, 2015).

Improvements in treatment options, e.g. surgical management and drugs with new therapeutic targets, resulted in a 15% decrease of the age-standardized death rate from cancer, but there are still cancer types with an unchanged poor prognosis. The tumour entity with the lowest 5-year relative survival in all stages is pancreatic cancer (11%) (Siegel et al., 2022).

Particularly, pancreatic cancer was the fourth leading cause for cancer-related death in the US in 2019 (Siegel et al., 2022) and it is estimated that by 2030 pancreatic cancer will rise to be the second leading cause (Rahib et al., 2014). Numerous reasons account for this poor development, including a lack of screening and prevention methods as well as very limited therapeutic approaches. Early and intermediate stages are treated with a combination of surgical removal and adjuvant or neoadjuvant chemotherapy according to the FOLFIRINOX-Protocol (combination of 5-fluorouracil/folic acid, irinotecan und oxaliplatin) (Conroy et al., 2018; Okusaka et al., 2020). Surgery alone is associated with poor outcome, therefore pharmacological treatment complements the therapy plan in all stages (Ryan, Hong, & Bardeesy, 2014). In advanced tumour stages, patients mostly receive palliative care, have an average survival of six to twelve months and are treated with chemotherapy and supportive care. Unfortunately, 80-85% of pancreatic cancers are detected in advanced disease stages with no curative treatment options left. Even when diagnosed in early stages and surgically removed, the 5-year-survival lies at 20-30% due to high rate of relapse (Ryan et al., 2014).

In summary, patients suffering from pancreatic cancer are still faced with few therapeutic alternatives and a poor prognosis. Chemo- or radiotherapy show only little success for pancreatic cancer, making it one of the most fatal malignancies (Adamska, Domenichini, & Falasca, 2017).

3.2 Precursor lesions of PDAC

Reliable screening methods were developed for various other cancer types. The basis for these early detection methods was the assumption of a stepwise progression, making it

possible to detect cancer at a non-malignant or non-invasive stage. In Germany, colonoscopy was already established in 2002 as screening method based on the concept of the colorectal adenoma-carcinoma sequence (Vogelstein et al., 1988).

In 2001, Hruban et al. first presented a histological model for PDACs, with 85% of cases the most common histological subtype of pancreatic cancer. It proposes a similar stepwise progression from defined precursor lesions towards invasive tissue (Hruban et al., 2001).

Currently, precursor lesions of PDAC are grouped in three types: pancreatic intraepithelial neoplasia (PanIN), intraductal papillary-mucinous neoplasm (IPMN) and mucinous cystic neoplasm (MCN) (Distler, Aust, Weitz, Pilarsky, & Grutzmann, 2014). Identifying these types correctly in human or mouse tissue and evaluating them according to their invasiveness is essential to assess the progression of pancreatic cancer. Disease stages can be monitored in premalignant states before the development of invasive tissue. This enables a more differentiated view on risk factors or the role of genetic alterations in the process of tumour formation. However, differential diagnosis of precursor lesions is difficult (Basturk et al., 2015; Hruban, Maitra, & Goggins, 2008) and the following criteria have to be considered for a reliable histological classification.

PanINs originate from smaller pancreatic ducts and measure less than 0.5 cm. (Hruban et al., 2008). PanIN lesions are categorized into three different grades: low-grade lesions (PanIN-1A (flat) and PanIN-1B (papillary)) are characterized through columnar epithelial cells with basally oriented uniform and round nuclei. Intermediate lesions (PanIN-2) have a higher grade of dysplasia, showing nuclear pleomorphism, nuclear crowding, nuclear hyperchromasia and loss of nuclear polarity. High-grade lesions (PanIN-3), also called “carcinoma in situ” (CIS), form complex papillary or cribiforme structures. The nuclei are enlarged, prominent and poorly oriented. They often show mitotic figures (Distler et al., 2014; Hruban et al., 2008). All PanINs do not infiltrate the basement membrane, making them non-invasive (Distler et al., 2014)

In contrary, IPMN lesions originate from main (MD-IPMN) or branch ducts (BD-IPMN). They show a rather cystic phenotype, are larger (> 1 cm) and more mucinous than PanIN lesions. They can be subclassified in low-grade, intermediate-grade and high-grade dysplasia and their genetic alterations mimic those of PanIN lesions (*LKRAS, p16, SMAD4, TRP53*) (Distler et al., 2014).

The main criterion is the size of the lesion (PanIN < 0.5 cm, IPMN > 1 cm), leaving the range between 0.5 to 1 cm to be either large PanINs or small IPMNs. Features like the morphological differentiation into intestinal, pancreatobiliary or oncocytic suggest IPMN lesions, while gastric-foveolar differentiation could indicate both, PanIN and IPMN lesions

(Basturk et al., 2015). The best way to differentiate those precursor lesions is their *GNAS* and *MUC* expression level (Basturk et al., 2015; Distler et al., 2014).

MCNs are easier to identify, as their pathology characteristically includes large cystic lesions with an underlying ovarian-type stroma, which shows positive immune staining for estrogen and progesterone. MCNs appear mostly in middle-aged women and are very rare findings (Matthaei, Schulick, Hruban, & Maitra, 2011).

In summary, the characterization of precursor lesions in pancreatic tissue samples can be utilized to compare the effects of different mutations on tumour progression and aggressiveness.

3.3 Genetic landscape of PDAC

In the past three decades, therapy strategies for PDAC changed from broad spectrum chemotherapy towards individual targeted therapy. The identification of oncogenes and their pathways has led towards the development of cancer driver inhibitors, such as vascular endothelial growth factor (VEGF)- or epidermal growth factor receptor (*EGFR)*-antibodies (Schneider, Schmidt-Supprian, Rad, & Saur, 2017). As pancreatic cancer still lacks these refined targeted therapies, the focus is turned toward profiling cancer drivers and creating new strategies to address this disease in the future.

The most frequent genetic abnormality in PDAC is the activation of oncogenic *KRAS*. The connection between mutant *KRAS* and cancer development has been investigated for decades (Almoguera et al., 1988; Smit et al., 1988) and nowadays members of the *RAS* superfamily, especially the isoform *KRAS*, are known as very common oncogenes (Drosten & Barbacid, 2020). KRAS mutations were detected in over 90 % of human PDAC tissue and is therefore the cancer type with the most frequent *KRAS* mutations, followed by colon (42 %) and lung (33 %) cancer (Simanshu, Nissley, & McCormick, 2017). Genetic alterations in PanIN precursor lesions are similar to those observed in invasive PDAC and a positive correlation between PanIN grade and the frequency of *KRAS2* gene mutations was found, showing 36% mutations of PanIN-1, 44% of PanIN-2 and 87% of PanIN-3 lesions (Lohr, Kloppel, Maisonneuve, Lowenfels, & Luttges, 2005). There is evidence, that only sustained mutational *KRAS* signalling is able to maintain PDAC (Brummelkamp, Bernards, & Agami, 2002) and switching off this oncogene puts tumour cells into a dormant state, waiting for *KRAS* reactivation (Eser, Schnieke, Schneider, & Saur, 2014). Moreover, molecular analysis revealed that two third of investigated mouse PDACs (mPDACs) showed an increased *Kras* gene dosage in former synchronized heterozygous mice. This was associated with increased metastatic potential (Mueller et al., 2018). *KRAS* was

deemed “undruggable” for a long time (Cox, Fesik, Kimmelman, Luo, & Der, 2014), but just recently a $KRAS^{G12C}$ inhibitor was presented with positive results in PDAC patients (Strickler et al., 2022).

Apart from *KRAS*, there are other common genetic alterations in PDAC inactivating tumour-suppressor genes like *CDKN2A*, *TP53*, *SMAD4* and *Tgfβ*, which are also detectable in intermediate- and high-grade PanIN precursor lesions. Even though somatic alterations do not have a strict order, some tend to appear before others. *KRAS2* and telomere shortening already appear in PanIN-1 stages, followed by *p16/CDKN2A* inactivation (PanIN-2) and finally *TP53* and *SMAD4* inactivation (PanIN-3) (Kanda et al., 2012). Recently it was discovered that they can also happen simultaneously in a catastrophic mitotic event (Mueller et al., 2018) and may not follow the initially described PDAC progression model (Notta et al., 2016).

Loss of SMAD 4 heterozygosity is observed in 90 %, homozygous deletion in 50 % of pancreatic carcinomas. In general, impaired SMAD signalling is associated with advanced disease, metastasis and poor prognosis (G. Yang & Yang, 2010). *SMAD4* is a mediator and key player of the transforming growth factor β (TGFβ) pathway and gene mutations of TGFβ-receptors or their pathway members are present in various cancer types, especially in gastrointestinal and pancreatic cancers (Korkut et al., 2018).

Jones et al described the TGFβ pathway as one of twelve core pathways, which are genetically altered in PDAC and downstream effectors like SMAD4 or TGFβ-receptor type II (TGFβRII) are representatives for these mutational changes (Jones et al., 2008).

3.4 TGFβ signalling

The TGFβ superfamily with over 33 members is organized into three groups: the TGFβ-, the activin-nodal- and the bone-morphogenetic-proteins-(BMP) subfamily (Goebel, Hart, McCoy, & Thompson, 2019).

The three TGFβ isoforms (TGFβ1, TGFβ2, TGFβ3) of the TGFβ-subfamily are synthesized in a latent form (L-TGFβ) with a propeptide region and the TGFβ protein (Daopin, Piez, Ogawa, & Davies, 1992; Schlunegger & Grutter, 1992).

L-TGFβ is bound by the latency associated peptide (LAP) to form the inactive small latent complex (SLC). The so-called latency lasso of LAP masks receptor-binding epitopes of TGFβ. Afterwards the SLC is bound by latent TGFβ binding protein (LTBP), forming a larger complex called large latent complex (LLC). Within the LLC, TGFβ is secreted into the extracellular matrix (ECM) (Rifkin, 2005).

Active TGFβ is released through the dissociation of LAP and TGFβ. This is the most critical step for signal activation and possibly facilitated by acidic pH, matrix metalloproteases or integrins. (Constam, 2014)

The active ligand then assembles two type I (activator) and two type II (signal-propagating) receptors, forming a hetero-tetrameric receptor complex. There are seven different type I and five type II transmembrane receptors in humans, but TGFβ binds exclusively to type I TGFβ-receptor (TGFβRI) and the TGFβRII, propagating its signal through the phosphorylation of serine or threonine residues (Massague, 2012). Later on, an additional tyrosine kinase activity in these receptors was discovered and effects on other non-canonical pathways were shown (Lawler et al., 1997).

Inside this hetero-tetrameric receptor complex, TGFβRII phosphorylates TGFβRI and the receptor complex can be either clathrin-dependently internalized, leading to an undisturbed *SMAD*-mediated pathway, or internalized via endocytosis through lipid rafts-caveolae with a degradation of the receptor-complex (Syed, 2016).

The *SMAD*-mediated pathway is also called the canonical pathway of TGFβ signalling. SMAD proteins consist of two domains, MH1 and MH2, which are connected by a linker. The MH1 domain contains a DNA-binding hairpin structure and the MH2 domain is in charge of binding various partners (Schmierer & Hill, 2007).

Phosphorylation of receptor-regulated SMADs (R-SMAD) through the TGFβ receptor complex creates an acid tail, capable of binding homologous MH2 sites. They bind the MH2 domain of SMAD4, a common SMAD (Co-Smad). A trimeric complex of two R-SMADs, in case of TGFβ SMAD2 and SMAD3, and one Co-SMAD is presumed to form a functional unit, which is able to pass through nucleoporins into the nucleus and regulate transcription. The hairpin of all SMADs bind to a gene site, which is the SMAD-binding element (SBE), consisting of the sequence CAGAC (Massague, 2012).

Known repressors of the canonical pathway are SMAD6 and 7, so-called inhibitory SMADs (I-SMADs). SMAD7 is localized inside the nucleus and represses TGFβ signalling in many ways. For example, it binds to the targeted DNA-site or moves to the cytosol to block interaction between R-SMADs and the receptor complex (Papageorgis, 2015). Moreover, SMAD7 is able to bind SMURF1 or SMURF2, initiating a SMURF-induced ubiquitination and henceforth degradation of the TGFβ-complex (Ebisawa et al., 2001).

Furthermore, the canonical pathway is strongly influenced by the cellular context. Both, intra- and extracellular variables, lead to diverging outcomes. For example, signal transduction changes through extracellular influences on the receptor-ligand-binding process. Density and arrangement of receptor subtypes or co-receptors and quantity of the predominant ligand isoforms and their receptor affinity determine the specific

proportion of different receptor-ligand-binding. So-called ligand trapping proteins can occupy the ligands binding region or anchor them, holding them in the extracellular matrix as for example described in individuals with marfan syndrome, resulting in a TGFβ release in the aortic wall and causing aneurysms (Holm et al., 2011). These factors, combined with further inhibitory or crosstalk inputs generate a unique signal transduction into the cell.

Intracellularly, the transcription of certain genes is influenced through the existence or absence of transcription factors, guiding the SMAD unit and resulting in positive or negative regulation, depending on which gene is targeted. Also, the epigenetic status of the genes, which makes them accessible or not to SMAD, plays an important role in determining signalling output (Massague, 2012).

Non-canonical signalling includes all pathways and effects, which are not mediated through activation of SMAD, since a variety of cross talks to other major pathways have been discovered enabling TGFβ to alter downstream cellular responses. These Non-SMAD pathways include for example MAPK-PI3K- (activated in cancer as oncogenes), WNT- (Facilitating epithelial to mesenchymal transition (EMT)), MYC- (cell proliferation) or PAR6-RhoGTPase-pathways (cell migration) (Zhang, 2009).

3.5 TGFβ in cancer

Even after decades of research, the role of TGFβ in cancer is not completely understood. The subsequent identification of TGFβ pathways and effector proteins made it possible to study their influence and behaviour in cancer cells.

In 1984 TGFβ was originally described as one of the most potent growth inhibitors (Tucker, Shipley, Moses, & Holley, 1984). Abolition of SMAD4 signalling in cancer is one of the first examples, indicating a tumour suppressive role of TGFβ. Moreover, TGFβRII is frequently mutated in patients with hereditary non-polyposis colorectal cancer, blocking proper signal transduction (Jakowlew, 2006) and lack of a functional TGFβRII allele (Wang et al., 1995) or overexpression of TGFβRII (Turco et al., 1999) in vitro caused growth inhibition in cancer cells. The ability of TGFβ to regulate cell cycle progression affirms its role as a tumour suppressor. The cell cycle is controlled by cyclin subunits and cyclin-dependent kinases (CDKs). They gather mitogenic and antiproliferative signals and progress or interrupt the cycle accordingly. Several CDK inhibitors act as tumour suppressors sending inhibitory signals to the cyclin/CDK-complexes. Expression levels of these inhibitors, especially p15 or p21, are enhanced by SMAD-dependent transcriptional activation. A SMAD-responsive element was found in a promoter of the proto-oncogene c-Myc, another crucial cell cycle protein, as it is able to regulate the transcription of many cell cycle related genes (Jakowlew, 2006).

Many in vitro and in vivo studies showed an increase in apoptosis through overexpression or treatment with TGFβ in various cell types like hepatocytes or epithelial cells (Larisch et al., 2000). The underlying mechanisms are only poorly understood in comparison to other pathways, but an influence on p53, Bcl-2 or caspase activity through TGFβ was found.
However, elevated TGFβ expression levels in cancer cells and enhanced invasiveness due to TGFβ1 overexpression challenge this one-sided view. The idea of a dual role in tumorigenesis arose. For instance, high levels of TGFβ isoforms in cancer patients blood (Picon, Gold, Wang, Cohen, & Friedman, 1998; Saito et al., 2000) and PDAC tissue (Friess et al., 1993; Wagner, Kleeff, Friess, Buchler, & Korc, 1999) correlate with poor prognosis. Other vital effects for cancer cell growth seem to be positively regulated by TGFβ like the alteration of microenvironment signalling, facilitating EMT, propagating immune evasion or recruitment of physiological resources (e.g. blood supply). Disruptions of the SMAD-dependent pathway seem to be critical for cancer cells to escape TGFβ-mediated growth arrest, suggesting that pro-tumorigenic effects are mostly mediated through non-canonical pathways. These escape mechanisms first need to be developed, implying a time-dependent role of TGFβ in tumorigenesis (Batlle & Massague, 2019; David & Massague, 2018).
Briefly, frequent loss-of-function mutations of TGFβ pathway members in both, hereditary and sporadic cancer types, apoptosis induction and cell cycle inhibition support the role of TGFβ as tumour suppressor. This seems to be the case in context of premalignant cells, but changes into a tumour promoter in more advanced stages (Massague, 2008). Exact mechanisms, underlying pathways and cooperation with the tumour microenvironment need to be further researched in the future.

3.6 Genetically engineered mouse models of PDAC

As mentioned above, KRAS mutations appear in over 90 % in human PDAC. (Simanshu et al., 2017). The first identified *RAS* downstream pathway was the mitogen-activated protein kinase (*MAPK*) pathway or *RAF-MEK-ERK* pathway. Soon after, the discovery of other *RAS* effectors followed and the links between *RAS* and numerous downstream targets indicated a variety of biological responses to *RAS* signalling, including cell proliferation, differentiation and survival (Malumbres & Barbacid, 2003).
Consequently, a reliable mouse model mirroring the progression of pancreatic cancer was developed using an oncogenic *Kras* allele at the endogenous locus. If *Kras* is bound to guanosine diphosphate (GDP) it remains inactive. Due to activation through guanosine exchange factor (GEF) it converts to its guanosine triphosphate (GTP)- bound form and is able to address its effector proteins (Bos, Rehmann, & Wittinghofer, 2007). Change of the

amino-acid glycine in position 12 of the Kras protein to aspartic acid (G12D) or to valine (G12V) leads to a permanent, GTP-independent activation of Kras and its downstream pathways. In PDAC mouse models the *Kras* allele is silenced by a loxP-stop-loxP (LSL) cassette and activated through the usage of Cre strains like Pancreatic and duodenal homebox 1-Cre (*Pdx1-Cre*) (Hingorani et al., 2003) or Pancreas Specific Transcription Factor 1-Cre (*Ptf1a-Cre*) (Kawaguchi et al., 2002). *Cre* strains lead to a recombination and thus deletion of the stop cassette in the *Kras* locus, resulting in an activation of oncogenic $Kras^{G12D}$ or $Kras^{G12V}$. While *Pdx1-Cre* is also expressed in the duodenum, *Ptf1a-Cre* is exclusively expressed in pancreatic cells (Collins & Pasca di Magliano, 2013). *Pdx1-Flp* is another site-specific recombinase, recognises *Frt* and activates specific genes with a Frt-stop-frt (FSF)-site (Theodosiou & Xu, 1998).

Analysis of this genetically engineered mouse model (GEMM) showed a similar development of PDAC compared to tumours evolving in humans regarding the histology of precursor lesions and tumour tissue (Hingorani et al., 2003), genetic instability and metastasis with a 70% rate of liver or lung metastasis (Guerra & Barbacid, 2013; Hingorani et al., 2003; Seidler et al., 2008).

By combining both recombinases (*Cre* and *Flp*), the resulting next-generation mouse-model is able to express different genes at once. Further development added a tamoxifen-inducible $CreER^{T2}$-strain to the mouse model, which can be used to activate the *Cre* recombinase, and therefore specific silenced gene sites, in a time-dependent manner (Schönhuber et al., 2014).

Consistent with the tumour suppressive role of TGFβ, in vivo studies with GEMM with additional defects of TGFβ signalling display more primary tumours with fastened progression, when confronted with various carcinogens. The combination of *Kras* and *Smad4* loss in mouse models also leads to fastened progression of PDAC compared to *Kras* alone (Bardeesy et al., 2006), while restauration of *Smad4* in vivo in these mice lead to delayed tumour growth (Duda et al., 2003). Furthermore, inhibition of TGFβ signalling reduced the number of metastases and lead to effective tumour control (Padua & Massague, 2009). Another mouse model with *TGFβRII* knockout has been reported to rapidly induce progression to PDAC in a *Kras* mutant background (Ijichi 2006). In summary, mouse models abrogating TGFβ signal transduction showed accelerated formation of metastatic PDAC and their clinical and histopathological manifestation recapitulated human PDAC (hPDAC).

3.7 Aim of this work

The aim of this thesis is to gain insights on the effects of TGFβ1 overexpression in PDAC initiation and progression. First, we characterized a GEMM with inherit oncogene *Kras*^{G12D} and constitutively active *TGFβ1* overexpression (PKTo) to evaluate the effect on PDAC tumour initiation in context of premalignant tissue. In total, 27 PKTo mice were histopathologically analysed. Three cell lines from this genetic background were cultivated and proliferation was determined by cell viability studies.

Second, we used a GEMM based on the dual-recombinase system (Schonhuber et al., 2014) with a tamoxifen-inducible time specific *Tgfβ1* overexpression (FKTo) in order to unravel the time-specific effects of *Tgfβ1* on pancreatic tissue. In our experimental setup FKTo mice were treated at different timepoints to induce *Tgfβ1* overexpression and histopathological outcome was determined in comparison to a control group.

4 Material and methods

4.1 Material

4.1.1 Technical equipment

Table 1: List of technical equipment

Device	Source
Analytical balance A 120 S	Sartorius AG, Göttingen
Analytical balance BP 610	Sartorius AG, Göttingen
Aperio AT2 Digital Whole Slide Scanner	Leica Microsystems GmbH, Wetzlar
Aperio Versa 8 Digital Scanner	Leica Microsystems Heerburg
Autoclave 2540 EL	Tuttnauer Europe B.V., Breda, The Netherlands
AxioCam HRc	Carl Zeiss AG, Oberkochen
AxioCam MRc	Carl Zeiss AG, Oberkochen
Centrifuge Rotina 46R	Andreas Hettich GmbH & Co. KG, Tuttlingen
CO_2 incubator HERAcell®	Heraeus Holding GmbH, Hanau
CO_2 incubator MCO-5AC 17AI	Sanyo Sales & Marketing Europe GmbH, Munich
Cryogenic Sample Storage	Worthington Industries, Cat# LS6000
Dewar carrying flask, type B	KGW-Isotherm, Karlsruhe
Gel Doc™ XR+ system	Bio-Rad Laboratories GmbH, Munich
Glass ware, Schott Duran®	Schott AG, Mainz
Heated paraffin embedding module EG1150 H	Leica Microsystems GmbH, Wetzlar
HERAsafe® biological safety cabinet	Thermo Fisher Scientific, Inc., Waltham, MA, USA
HERA freeze™	HFU T Series, Thermo Scientific™, Cat# HFU500TV
Horizontal gel electrophoresis system	Biozym Scientific GmbH, Hessisch Oldenburg
Horizontal shaker	Titertek Instruments, Inc., Huntsville, AL, USA
Incubator shaker Thermoshake	C. Gerhardt GmbH & Co. KG, Königswinter
Laminar flow HERAsafe	Heraeus Holding GmbH, Hanau
Magnetic stirrer, Ikamag® RCT	IKA® Werke GmbH & Co. KG, Staufen
Microcentrifuge 5415 D	Eppendorf AG, Hamburg
Microcentrifuge 5417 R	Eppendorf AG, Hamburg
Microplate reader Anthos 2001	Anthos Mikrosysteme GmbH, Krefeld
Microscope Axio Imager.A1	Carl Zeiss AG, Oberkochen
Microscope Axiovert 25	Carl Zeiss AG, Oberkochen
Microscope DM LB	Leica Microsystems GmbH, Wetzlar
Microtome Microm HM355S	Thermo Fisher Scientific, Inc., Waltham, MA, USA
Microwave	Siemens AG, Munich
Mini centrifuge MCF-2360	LMS Consult GmbH & Co. KG, Brigachtal

Device	Source
Multipette® stream	Eppendorf AG, Hamburg
Neubauer hemocytometer, improved	LO-Laboroptik GmbH, Bad Homburg
Paraffin tissue floating bath Microm SB80	Thermo Fisher Scientific, Inc., Waltham, MA, USA
Pipettes Reference®, Research®	Eppendorf AG, Hamburg
Pipetus®	Hirschmann Laborgeräte GmbH & Co. KG, Eberstadt
Power supplies E844, E822, EV243	Peqlab Biotechnologie GmbH, Erlangen
Surgical instruments	Thermo Fisher Scientific, Inc., Waltham, MA, USA
Thermocycler T1	Biometra GmbH, Göttingen
Thermocycler Tgradient	Biometra GmbH, Göttingen
Thermocycler Tpersonal	Biometra GmbH, Göttingen
Thermocycler UNO-Thermoblock	Biometra GmbH, Göttingen
Thermomixer compact	Eppendorf AG, Hamburg
Tissue processor ASP300	Leica Microsystems GmbH, Wetzlar
Tumbling Table WT 17	Biometra GmbH, Göttingen
Vortex Genius 3	IKA® Werke GmbH & Co. KG, Staufen
Water bath 1003	GFL Gesellschaft für Labortechnik mbH, Burgwedel

4.1.2 Disposables

Table 2: List of disposables

Disposable	Source
Cell culture plastics	Becton Dickinson GmbH, Franklin Lakes, NJ, USA; Greiner Bio-One GmbH, Frickenhausen; TPP Techno Plastic Products AG, Trasadingen, Switzerland
Cell scrapers	TPP Techno Plastic Products AG, Trasadingen, Switzerland
Combitips BioPur®	Eppendorf AG, Hamburg
Conical tubes, 15 ml	TPP Techno Plastic Products AG, Trasadingen, Switzerland
Conical tubes, 50 ml	Sarstedt AG & Co., Nümbrecht
Cover slips	Gerhard Menzel, Glasbearbeitungswerk GmbH & Co. KG, Braunschweig
CryoPure tubes	Sarstedt AG & Co., Nümbrecht
Disposable scalpels, size 11 and 21	Feather Safety Razor Co., Ltd., Osaka, Japan
Glass slides Superfrost® Plus	Gerhard Menzel, Glasbearbeitungswerk GmbH & Co. KG, Braunschweig
MicroAmp® optical 96-well reaction plate	Applied Biosystems, Inc., Carlsbad, CA, USA

Disposable	Source
Microtome blades S35 and C35	Feather Safety Razor Co., Ltd., Osaka, Japan
Parafilm™	M Laboratory Wrapping Film, Bemis™, Cat# 9170005
PCR reaction tubes	Brand GmbH + Co. KG, Wertheim; Eppendorf AG, Hamburg
Petri dishes	Sarstedt AG & Co., Nümbrecht
Phase lock gel light tubes	5 Prime GmbH, Hamburg
Pipette tips	Sarstedt AG & Co., Nümbrecht
Reaction tubes, 0.5 ml, 1.5 ml and 2 ml	Eppendorf AG, Hamburg
Safe seal pipette tips, professional	Biozym Scientific GmbH, Hessisch Oldenburg
Safe-lock reaction tubes BioPur®	Eppendorf AG, Hamburg
Serological pipettes	Sarstedt AG & Co., Nümbrecht
Single use needles Sterican® 27 gauge	B. Braun Melsungen AG, Melsungen
Single use syringes Omnifix®	B. Braun Melsungen AG, Melsungen
Tissue embedding cassette system	Medite GmbH, Burgdorf

4.1.3 Reagents and enzymes

Table 3: List of common reagents and enzymes

Reagent	Source
2-Mercaptoethanol, 98%	Sigma-Aldrich Chemie GmbH, Munich
Acetic acid (glacial)	Merck KGaA, Darmstadt
Agarose	Sigma-Aldrich Chemie GmbH, Munich
Ammonium persulfate	Sigma-Aldrich Chemie GmbH, Munich
Bovine serum albumin, fraction V	Sigma-Aldrich Chemie GmbH, Munich
Buffer S, 10x	VWR International, Radnor, PA, USA
Cresol red	Sigma-Aldrich Chemie GmbH, Munich
Dimethylsulfoxide (DMSO)	Carl Roth GmbH + Co. KG, Karlsruhe
dNTP mix, 10mM each	Fermentas GmbH, St. Leon-Rot
Ethanol (100%)	Merck KGaA, Darmstadt
Ethidium bromide	Sigma-Aldrich Chemie GmbH, Munich
Ethylenediaminetetraacetic acid (EDTA)	Invitrogen GmbH, Karlsruhe
Gel loading dye, blue	New England Biolabs GmbH, Frankfurt am Main
GeneRuler™ 100bp DNA ladder	Fermentas GmbH, St. Leon-Rot
Glycerol	Sigma-Aldrich Chemie GmbH, Munich
HotStarTaq DNA polymerase	Qiagen GmbH, Hilden
Hydrochloric acid (HCl)	Merck KGaA, Darmstadt
Isotonic sodium chloride solution	Braun Melsungen AG, Melsungen
Magnesium chloride	Carl Roth GmbH + Co. KG, Karlsruhe

Reagent	Source
Methanol	Merck KGaA, Darmstadt
Peanut oil	Sigma-Aldrich Chemie GmbH, Munich
Dulbecco's phosphate buffered saline (PBS)	Invitrogen GmbH, Karlsruhe
Dulbecco's phosphate buffered saline, powder	Biochrom AG, Berlin
Proteinase K, recombinant, PCR grade	Roche Deutschland Holding GmbH, Grenzach-Wyhlen
REDTaq® ReadyMix™ PCR reaction mix	Sigma-Aldrich Chemie GmbH, Munich
Sodium acetate buffer solution	Sigma-Aldrich Chemie GmbH, Munich
Sodium chloride (NaCl)	Merck KGaA, Darmstadt
Sodium hydroxide solution (NaOH)	Merck KGaA, Darmstadt
Sucrose (saccharose)	Merck KGaA, Darmstadt
Tamoxifen	Sigma-Aldrich Chemie GmbH, Munich
Tamoxifen chow CreActive TAM400	LASvendi, Soest
Tris hydrochloride	J.T.Baker® Chemicals, Phillipsburg, NJ, USA
Tris Pufferan®	Carl Roth GmbH + Co. KG, Karlsruhe
Triton® X-100	Merck KGaA, Darmstadt

Table 4: List of reagents and enzymes for cell culture

Reagent	Source
Collagenase type 2	Worthington Biochemical Corporation, Lakewood, NJ, USA
Dulbecco's modified eagle medium (DMEM) with L-glutamine	Invitrogen GmbH, Karlsruhe
Fetal calf serum (FCS)	Biochrom AG, Berlin
Giemsa solution	Sigma-Aldrich Chemie GmbH, Munich
MTT Reagent	Sigma-Aldrich Chemie GmbH, Munich
Penicillin (10000 units/ml) / Streptomycin (10000 µg/ml) solution	Invitrogen GmbH, Karlsruhe
Trypsin, 0.05% with 0.53 mM EDTA 4Na	Invitrogen GmbH, Karlsruhe

Table 5: List of reagents and enzymes for histology and immunohistochemistry (IHC)

Reagent	Source
Antigen unmasking solution, citric acid based	Vector Laboratories, Inc., Burlingame, CA, USA
Avidin/biotin blocking kit	Vector Laboratories, Inc., Burlingame, CA, USA
Eosine	Waldeck GmbH & Co KG, Münster
Haematoxylin	Merck KGaA, Darmstadt
Histosec® pastilles (without DMSO)	Merck KGaA, Darmstadt
Hydrogen peroxide 30%	Merck KGaA, Darmstadt
Pertex mounting medium	Medite GmbH, Burgdorf
Roti® Histofix 4%	Carl Roth GmbH + Co. KG, Karlsruhe
Roti® Histol	Carl Roth GmbH + Co. KG, Karlsruhe
Tween® 20	Carl Roth GmbH + Co. KG, Karlsruhe

4.1.4 Solutions

Table 6: List of Solutions

Solutions	Source
SucRot solution	1.5 mg/mL Cresol red 100 mM Tris, pH 9.0 30 % saccharose
Soriano lysis buffer	0.5 % Triton® X-100 1 % 2-Mercaptoethanol 1× Gitschier’s buffer 400 µg /mL Proteinase K (add prior to use)
Gitschier’s buffer, 10×	670 mM Tris, pH 8.8 166 mM (NH4)2SO4 67 mM MgCl2
PBST	0.1% Tween® 20 in PBS
Tris acetate EDTA (TAE) buffer, pH 8.5, 50×	2 M Tris 50 mM EDTA 5.71% Acetic acid

Table 7: Cell culture media and their components

Medium	Components
Cancer cell medium	DMEM 10% FCS (Biochrom AG) 1% Penicillin/Streptomycin
Freezing medium	70% DMEM 20% FCS 10% DMSO

4.1.5 Antibodies

Table 8: Primary antibodies for IHC

Reagent/ kit	Source
CK19 TROMA-III (primary Antibody)	Developmental Studies Hybridoma Bank, rat, Cat# TROMA-III, RRID:AB_2133570
Ki67 (SP6) (primary Antibody)	DCS, rabbit, Cat# KI681C01

Table 9: Secondary antibodies for IHC

Reagent/ kit	Source
Biotinylated anti-rabbit IgG (H+L)	Vector Laboratories, Inc., Burlingame, CA, USA
Biotinylated anti-rat IgG (H+L)	Vector Laboratories, Inc., Burlingame, CA, USA

4.1.6 Primers

Table 10: Primers used for genotyping

PCR name	Primer name	Sequence (5´ → 3´)
Pdx1-Flp	Pdx1-Flp forward	AGAGAGAAAATTGAAACAAGTGCAGGT
	Flp reverse	CGTTGTAAGGGATGATGGTGAACT
	Gabra forward (Ctrl)	AACACACACTGGAGGACTGGCTAGG
	Gabra reverse (Ctrl)	CAATGGTAGGCTCACTCTGGGAGATGATA
FSF-Kras^{G12D}	FSF-Kras common forward	CACCAGCTTCGGCTTCCTATT
	FSF-Kras WT reverse	AGCTAATGGCTCTCAAAGGAATGTA
	FSF-Kras MUT reverse	GCGAAGAGTTTGTCCTCAACC
FSF-Kras^{G12D} del	FSF-Kras del forward	AGAATACCGCAAGGGTAGGTGTTG
	FSF-Kras del reverse	TGTAGCAGCTAATGGCTCTCAAA
CreERT2	CreERT2 forward (*R26CAG-CreERT2* line)	GAATGTGCCTGGCTAGAGATC
	CreERT2 reverse (*R26CAG-CreERT2* line)	GCAGATTCATCATGCGGA
	CreERT2 recombined reverse	CGATCCCTGAACATGTCCATC
R26-CAG	R26 common forward	AAAGTCGCTCTGAGTTGTTAT
	R26 WT reverse	GGAGCGGGAGAAATGGATATG
	R26CAG-CreERT2 MUT reverse	TCAATGGGCGGGGGTCGTT
Frt-stop-Frt	FSF forward	TGAATAGTTAATTGGAGCGGCCGCAATA
	FSF reverse	CAGGGTGTTATAAGCAATCCC
FSF-Cre stop del	FSF-Cre stop del forward	GTTCGGCTTCTGGCGTGT
	FSF-Cre stop del reverse	CGATCCCTGAACATGTCCATC

PCR name	Primer name	Sequence (5´ → 3´)
$Ptf1a^{Cre}$	Ptf1a-Cre-GT-LP-URP	CCTCGAAGGCGTCGTTGATGGACTGCA
	Ptf1a-Cre-GT-wt-UP	CCACGGATCACTCACAAAGCGT
	Ptf1a-Cre-GT-mut-UP-neu	GCCACCAGCCAGCTATCAA
LSL-$Kras^{G12D}$	LSL-Kras common forward	CACCAGCTTCGGCTTCCTATT
	LSL-Kras WT reverse	AGCTAATGGCTCTCAAAGGAATGTA
	LSL-Kras MUT reverse	CCATGGCTTGAGTAAGTCTGC
LSL-$R26^{TGF\beta/+}$	R26-Tva-GT-UP	AAAGTCGCTCTGAGTTGTTAT
	R26-Tva-GT-wt_LP	GGAGCGGGAGAAATGGATATG
	FsaSFneosa_LP2	ATTGCATCAGCCATGATGGATACTTTCT
LSL-$R26^{TGF\beta/+}$ rec stop	Soriano SA UP	CAG TAG TCC AGG GTT TCC TTG ATG
	mTGFβ1 LP	GCTGATCCCGTTGATTTCC
	pgl3-pa-pause 4645 UP	TGAATAGTTAATTGGAGCGGCCGCAATA
LSL-$Rosa26^{TGF\beta/+}$ gene	mTGFβ1 UP	AGGTCACCCGCGTGCTAAT
	mTGFβ1 LP	GCTGATCCCGTTGATTTCC

4.1.7 Software

Table 11: Software

Software	Source
Adobe Illustrator CS	Adobe Inc, USA
Aperio Image Scope v12.3	Leica Biosystems, Wetzlar
AxioVision 4.8	Carl Zeiss AG, Oberkochen
Excel	Microsoft Corporation, Redmont, WA, USA
GraphPad Prism 9	La Jolla, CA, USA

4.2 Methods

4.2.1 Mouse experiments

All animal studies were conducted according to the european guidelines for the care and use of laboratory animals and approved by the local authorities.

4.2.1.1 Mouse strains

Mouse models harbouring the *Cre/loxP*- or *Flp/frt*-system were used in this study. Genes, which are flanked by *loxP* or *frt* can be deleted through combination with a tissue-specific expression of *Cre* or *Flp* recombinase. This yields the possibility to either inactivate a gene through direct deletion or activate it through deletion of the corresponding Stop-cassette.

***Ptf1a*$^{Cre/+}$** (Nakhai et al., 2007). This knock-in mouse strain was kindly provided by Dr. Hassan Nakhai (Klinikum rechts der Isar, Technical University Munich). Pancreas transcription factor 1 subunit alpha (*Ptf1a*) is expressed in pancreatic tissue and plays a role in its development. The *Cre* recombinase is under the control of the *Ptf1a* promoter and therefore exclusively expressed in pancreatic tissue.

***LSL-Kras*$^{G12D/+}$** (Jackson et al., 2001; Yao et al., 2003). This knock-in mouse strain was kindly provided by Prof. Tyler Jacks (Massachusetts Institute of Technology, Cambridge, MA, USA). These mice carry oncogenic *Kras* with a point mutation in codon 12, which leads to an amino acid substitution of glycine by aspartate. This mutation is frequently observed in pancreatic cancer in humans and results in a permanently activated GTPase activity of KRAS. Deletion of the *loxP*-flanked Stop codon through *Cre* recombinase activates oncogenic *Kras*.

***LSL-R26*$^{Tgfβ/+}$** (Hieber, 2021) This transgenic mouse strain was generated in the laboratory of Prof. Dieter Saur. An *LSL-Tgfβ1-pA*-casette was implanted in the Rosa26 locus of murine embryonal stem cells. Those recombined cells were injected into C57BL6/J blastocysts, generating chimeric mice. The resulting mice carried *the LSL-R26*$^{TGFβ/+}$ genotype, where *Tgfβ1* is silenced by *an LSL*-Stop-cassette.

Pdx1-Flp (Schönhuber et al., 2014). This transgenic mouse strain was generated in the laboratory of Prof. Dieter Saur. The *Flp* recombinase is active under the pancreas specific *Pdx1* promoter.

FSF-Kras$^{G12D/+}$ (Schönhuber et al., 2014). This knock-in mouse strain was generated in the laboratory of Prof. Dieter Saur. Oncogenic *Kras* is silenced through a *frt*-flanked Stop-cassette and can be activated with active *Flp* recombinase.

FSF-R26$^{CAG\text{-}CreERT2/+}$ (Schönhuber et al., 2014). This mouse strain was generated in the laboratory of Prof. Dieter Saur. The latent tamoxifen-inducible *CreERT2* can be used to activate *Cre* recombinase in a time-dependent manner.

Tgfbr2$^{lox/lox}$ (Ijichi et al., 2006). This transgenic mouse strain was generated in the laboratory of Prof. Dieter Saur. Homozygous knockout of the TGFβRII leads to impaired TGFβ signalling.

Three different GEMMs harbouring the *LSL-R26$^{Tgf\beta/+}$* overexpression allele and corresponding control groups without *LSL-R26$^{Tgf\beta/+}$* were characterized in this study. Abbreviations are used in the following chapters as listed in Table 12:

Table 12: Nomenclature of mouse lines

PTo	*Ptf1a$^{Cre/+}$*, ***LSL-R26$^{Tgf\beta/+}$***
PKTo	*Ptf1a$^{Cre/+}$*, *LSL-Kras$^{G12D/+}$*, ***LSL-R26$^{Tgf\beta/+}$***
FKTo	*Pdx1-Flp, FSF-Kras$^{G12D/+}$*, *FSF-R26$^{CAG\text{-}CreERT2}$*, ***LSL-R26$^{Tgf\beta/+}$***
PK	*Ptf1a$^{Cre/+}$*, *LSL-Kras$^{G12D/+}$*
PKT-HOM	*Ptf1a$^{Cre/+}$*, *LSL-Kras$^{G12D/+}$*, *Tgfbr2$^{lox/lox}$*

4.2.1.2 Genotyping

All mice were genotyped twice (2-3 weeks after birth and after death) to confirm the correct genotype. A 1 mm long tail biopsy was taken from 2-3 weeks old mice with a sterile scalpel. Each mouse got an explicit ear marking representing their number code. The DNA was extracted as described in 4.2.4.1 Isolation of DNA. The same DNA extraction and genotyping procedure was repeated with a 2-3 cm long tail after being sacrificed.

4.2.1.3 Tamoxifen treatment of mice

To analyse if the activation of TGFβ during different timepoints leads to different outcomes in tumour formation and progression, TGFβ was activated through tamoxifen treatment in mice at the age of three and six months.

The treatment protocol had a three-weeks-schedule: First, mice were fed with Tamoxifen-containing food (400 mg tamoxifen citrate per kg food; LASvendi, Soest) for one week.

Subsequently, they received normal food for one week, as they often presented with worsened health conditions and body weight (BW) loss. The third week the mice got two intraperitoneal (i.p.) injections with 4 mg of tamoxifen dissolved in peanut oil supplemented with 10 % ethanol. The dosage was BW dependent. If the mouse weight was under 25 g, they got a dosage of 0.4 mL/gBW, if the body weight was over 25 g they received 0.6mL/gBW.

All mice were monitored during the Tamoxifen treatment regarding their health condition and body weight and stress burden was assessed daily under exposition.

4.2.1.4 Mouse dissection

The mice were anaesthetized with a body weight adapted i.p. injection of MMF (5 mg/kg midazolam, 500 µg/kg medetomidine, 50 µg/kg fentanyl). After the loss of their reflexes mice were euthanized, the abdomen disinfected with 70 % ethanol and cut open. Samples were taken as sterile as possible.

Small pieces of pancreatic tissue were taken for further analysis. Tissue for DNA and RNA extraction was immediately snap-frozen and stored at -80°C until further use. Another piece of pancreatic tumour was taken for generating cell lines (see 4.2.3.1 Generation and culture of primary mouse PDAC cell lines).

The rest of the pancreas, spleen, liver, lung, heart, kidneys and stomach was removed, washed in PBS, weighted and fixed for 24 h with 4 % Roti® Histofix.

4.2.2 Histological analysis

4.2.2.1 Paraffin sections

The organs for histological analysis were fixed for 24 h with 4 % Roti® Histofix, washed with PBS, dehydrated using the tissue processor ASP300, embedded in paraffin and stored at room temperature (RT) until further use.

For following staining, the tissue was cut into 0.5-1 µm thick sections with the microtome Microm HM355S.

4.2.2.2 Hematoxylin and eosin staining of tissue sections

Paraffin-embedded sections were dewaxed with Roti® Histol (incubation 2 x 5 min), After that, the sections were rehydrated in a decreasing ethanol series (2 x 99 %, 2 x 96 % and 2 x 80 %; 2-3 min each) and rinsed with water. The slides were placed into haematoxylin for 20 s, then washed with tap water for 2-3 min, until the water did not show any traces of haematoxylin.

The sections were placed into eosin for 20 s, then washed with distilled water.

The sections were dehydrated with an increasing ethanol series (2 x 80 %, 2 x 96 % and 2 x 99 %; 2-3 min each) and incubated in Roti® Histol (2 x 5 min) before they were covered with Pertex mounting medium.

4.2.2.3 Immunohistochemistry

Paraffin-embedded sections were dewaxed and rehydrated as described in 4.2.2.1 Paraffin sections. Subsequently, they were boiled in citric-acid-based antigen unmasking solution in a microwave at 360 W for 10 min. After cooling down for at least 20 min, the sections were rinsed with water. To inhibit endogenous peroxidase activity, they were incubated with 3 % H_2O_2 for 15 min in the dark. After that, the sections were first washed with water, then three times with PBS and blocked with PBST containing 5 % serum for 1 h at RT. The sections were washed three times with PBS again and incubated with the primary antibody ck19 (TROMA-III, rat, dilution 1:300) or ki67 (SP6, rabbit, dilution 1:50), respectively, diluted in 3-5 % serum in PBS overnight at 4°C.

After incubation they were washed three times with PBS and incubated with the secondary antibody (anti-rabbit or anti-rat, dilution 1:500) diluted in 3-5 % serum in PBS for 1 h at RT. Slides were washed again, dehydrated, counterstained with haematoxylin and mounted as described in 4.2.2.2 Hematoxylin and eosin staining of tissue sections.

4.2.2.4 Analysis of stained slides

Slides were photographed using a bright-field microscope connected to a camera or slide scanner.

Organs (pancreas, liver, lung) were screened for primary tumour and metastasis. For this purpose, organs were cut into 3 serials with an interval of 150 µm, each serial containing 2-4 slides with a thickness of 0.5-1 µm.

PanIN lesions were quantified in timepoint mice. For each timepoint (three, six, nine and twelve month), three different mice were used with one representative slide per mouse. Ki67-positive cells were counted in tumour mice with 10 fields of view of one representative slide per mouse.

4.2.3 Cell culture experiments

Primary cancer cells were taken from tumour mice and cultivated. All conditions were kept as sterile as possible. The composites of cell culture media are shown in Table 7.

4.2.3.1 Generation and culture of primary mouse PDAC cell lines

A piece of pancreatic tumour was first washed in sterile PBS, then cut into very small pieces with a sterile scalpel and diluted with 5 ml of cancer cell medium (DMEM

supplemented with 10 % FCS and 1 % P/S) supplemented with 200 U/mL collagenase type 2 under a biological safety cabinet. Afterwards it was incubated at 37°C for 24-48 h. After incubation, the cell suspension was centrifuged for 5 min with 1200 rpm. The resulting pellet was taken, dissolved in 5 ml cancer cell medium and moved to a small cell culture flask (25 cm^2).

For passaging of the cells, old medium was aspirated, cells were washed 2-3 times with 5 ml sterile PBS and detached from the bottom of the flask with trypsin/EDTA at 37°C for 2-4 minutes. The trypsinization was stopped through addition of cancer cell medium.

The cell suspension was seeded into a new vessel according to further planned experiments.

The cell number was counted, if needed, with a Neubauer hemacytometer.

For cryopreservation, the cell suspension was centrifuged at 1200 rpm for 5 min and the pellet was dissolved in ice-cold freezing medium (70 % DMEM supplemented with 20 % FCS and 10 % DMSO). Subsequently, the suspension was moved to CryoPure tubes, frozen at -80°C for 24 h and afterwards stored in liquid nitrogen.

Cell morphology was documented with a bright-field microscope connected to a camera.

4.2.3.2 MTT assay

The MTT assay is used to determine the viability of cells and was performed on days one, three and five after seeding to measure cell proliferation. Yellow 3-(4,5-Dimethyl-2-thiazolyl)-2,5-diphenyl-tetrazolium bromide (MTT) is added and the cells convert MTT into dark blue formazan crystals by NADH-dependent reductases.

100 µL of cancel cell medium containing 500 cells per well was seeded in a 96-well-plate with three replicates for each cell line. 10 µL of MTT reagent were added, resulting in a final concentration of MTT dye of 0.5 mg/mL and incubated for 4 h at 37°C. Afterwards, cell medium was removed, the formazan crystals were dissolved with 200 µL of an ethanol / DMSO mix (1:1) and the 96-well-plate was shaken for 10 min at RT.

The optical density of the samples was determined by the plate spectrophotometre Anthos 2001 at a wavelength of 600 nm.

4.2.3.3 Clonogenic assay

2000 cells per well were seeded on a 6-well-plate. Cells were fixed after 6 days by removing cancer cell medium and adding cold 99 % methanol, while shaking for 30 min at RT. Colonies were stained with Giemsa solution (diluted 1:20 in distilled water) after removal of methanol on an orbital shaker overnight. The next day, Giemsa solution was removed, plates were washed with distilled water and air dried.

4.2.4 Molecular biology

4.2.4.1 Isolation of DNA

DNA of tissue samples or cell pellets was isolated by adding 50-200 µL of Soriano lysis buffer and put into a thermocycler at 55°C for 90 min. Proteinase K was heat inactivated for 15 min at 95 °C. Afterwards, all samples were vortexed and centrifuged at 14000 rpm and 4°C for 10 min. The DNA-containing supernatant was transferred into a new tube and stored at either 4°C for a short time or at -20°C for a longer time period until further use.

4.2.4.2. Polymerase chain reaction (PCR)

For genotyping or recombination PCR a standard PCR reaction setup was used, as shown in Table 14. The composites of the PCR pre-mix are shown in Table 13. PCR products were stored at 4°C until further analysis by gel electrophoresis.

Table 13. Composition of pre-mix for PCR.

Solution	**Volume for one reaction**
ddH_2O	4.375 µL
10 x buffer S	2.5 µL
30 % sucrose	2.5 µL
SucRot	2.5 µL
PeqTaq	0.125 µL
dNTPs (10 µM each)	0.5 µL

Table 14. Reaction mix and conditions for standard PCR.

Reaction Mix		**Conditions**		
12.5 µL	PCR pre-mix	95°C	3 min	
0.25 - 2 µL	forward primer (10 µM)	95°C	45 s	40x
0.25 - 2 µL	reverse primer (10 µM)	55°C – 72°C	60 s	
1.5 µL	DNA	72°C	90s	
ad 25 µL	H_2O	25°C	hold	

For genotyping PCR tail DNA of a mouse was taken and isolated as described in 4.2.4.1 Isolation of DNA. For recombination PCR either small samples of pancreatic tissue or cell pellets were taken.

Table 15. Annealing temperatures and PCR products of genotyping and recombination PCRs.

Name of PCR	Annealing temperature	PCR products (bp)
Pdx1-Flp	55°C	620 (mut) / 300 (internal control)
FSF-Kras^{G12D}	55°C	350 (mut) / 270 (WT)
FSF-Kras^{G12D} del	60°C	196 (rec)
FSF-Stop	60°C	600 (mut)
FSF-R26-CreERT2	55°C	190 (mut)
FSF-R26-CAG	62°C	450 (mut) / 650 (WT)
FSF-Cre stop del	60°C	490 (rec)
Ptf1a^{Cre}	60°C	400 (mut) / 600 (WT)
LSL-Kras^{G12D}	55°C	170 (mut) / 270 (WT)
LSL-R26TGFβ/+	58°C	851 (mut) / 600 (R26 WT)
LSL-R26TGFβ/+ rec stop	58°C	885 (del), 1022 (not del)
LSL-R26TGFβ/+ gene	55°C	400 (mut)

mut = mutated allele; WT = wild type allele; rec = mutated allele without translational stop element after recombination

4.2.4.3. Agarose gel electrophoresis

Agarose gels were prepared with a concentration of 1.5-2 %. Diluted TAE Buffer (1x) and agarose were boiled in a microwave and continuously mixed with a magnetic stirrer. When cooled to approximately 60 °C ethidium bromide was added and the gel was poured into a chamber with combs. Combs were removed after gel was cooled down and solid.

PCR products were pipetted into the wells and separated at 100 V in TAE buffer (1x). Bands were visualized via UV light and pictures were taken with the GEL Doc XR+ system.

4.2.5 Statistical analysis

Data analysis was performed with GraphPad Prism 9. All data were obtained from three independent experiments, unless declared otherwise. It was analysed as mean values ± standard deviation (SD). A p-value of < 0.05 was considered statistically significant. Regarding cell culture experiments, MTT assay was performed in triplicates and clonogenic assay in quadruples. Histological evaluation was done with three replicates and one representative slide. Kaplan-Meier-estimator was used for survival analysis.

5 Results

5.1 Overexpression of Tgfβ1 in a $Kras^{G12D}$-driven PDAC mouse model leads to distinct histopathological phenotypes

To analyse the influence of *Tgfβ1 overexpression* on PDAC initiation, our lab generated the constitutively active *Tgfβ1* overexpression allele *LSL-R26$^{TGF\beta/+}$(Hieber, 2021)*. Since *Kras* mutations are found in over 90 % of human PDAC tissue and are already present in early PDAC precursor lesions (Kanda et al., 2012), it has been shown, that mice with oncogenic *Kras^{G12D}*, referred to as PK-mice or control, respectively, proofed to be a reliable mouse model of hPDAC (Hingorani et al., 2003) Therefore, a PDAC model with combined pancreas-specific, simultaneous activation of oncogenic *Kras^{G12D}* and *Tgfβ1* (PKTo) was investigated (Figure 1A). Their genotype was confirmed as described in 4.2.4.2. Polymerase chain reaction (PCR) and depicted in Figure 1B.

PK mice develop ductal lesions with complete penetrance (Hingorani et al., 2003) and show a variety of differentiated to undifferentiated tumour phenotypes, graded into four stages (G1-G4). The development towards undifferentiated types is depending on their mutagen *Kras* gene-dosage (Mueller et al., 2018). In contrast, histopathological analysis of PKTo pancreata showed a mixture of cystic papillary lesions and low-grad PanIN lesions up to PanIN-2, sometimes flanked by intact pancreatic acini in 85,2 % of cases. Only a small fraction of 14.8 % (n=4) presented a solid tumour mass, which was histologically undifferentiated to G3 or G4 as displayed in Figure 1E and Figure 2A.

Subsequently, PKTo mice were histopathological classified into two distinct subtypes with either cystic histopathological phenotype (PKTo-CYS) or invasive carcinoma (PKTo-SOL). Ki67 staining of the pancreata confirmed a significantly higher proliferation rate of PKTo-SOL pancreatic tissue compared to PKTo-CYS mice, as shown in Figure 1F. The proliferation rate of PKTo-SOL tumours was comparable to the proliferation rate of dedifferentiated carcinoma (grading G4) of PK mice.

Notably, all PKTo-SOL mice showed metastasis formation either in liver, lungs or both organs as displayed in Figure 2B, which is also similar to undifferentiated PK tumours (Mueller et al., 2018).

Nonetheless, PKTo-SOL and PKTo-CYS mice with and without PDAC formation showed a significantly reduced median survival (298 days and 356.5 days) compared to the PK control (433.5 days) as shown in Figure 1D.

In summary, *Tgfβ1* overexpression in *Kras^{G12D}*-driven PDAC leads to two different phenotypes suggesting distinct evolutionary routes of tumorigenesis, which need to further be investigated. Interestingly, the majority of tumour cases display a cystic phenotype

without PDAC formation indicating a tumour suppressive role of *Tgfβ1* overexpression. In contrast, the few cases of invasive carcinoma formation imply a tumour promoting role. Therefore, it is important to perform genomic analysis to understand the genetic basis of these two phenotypes.

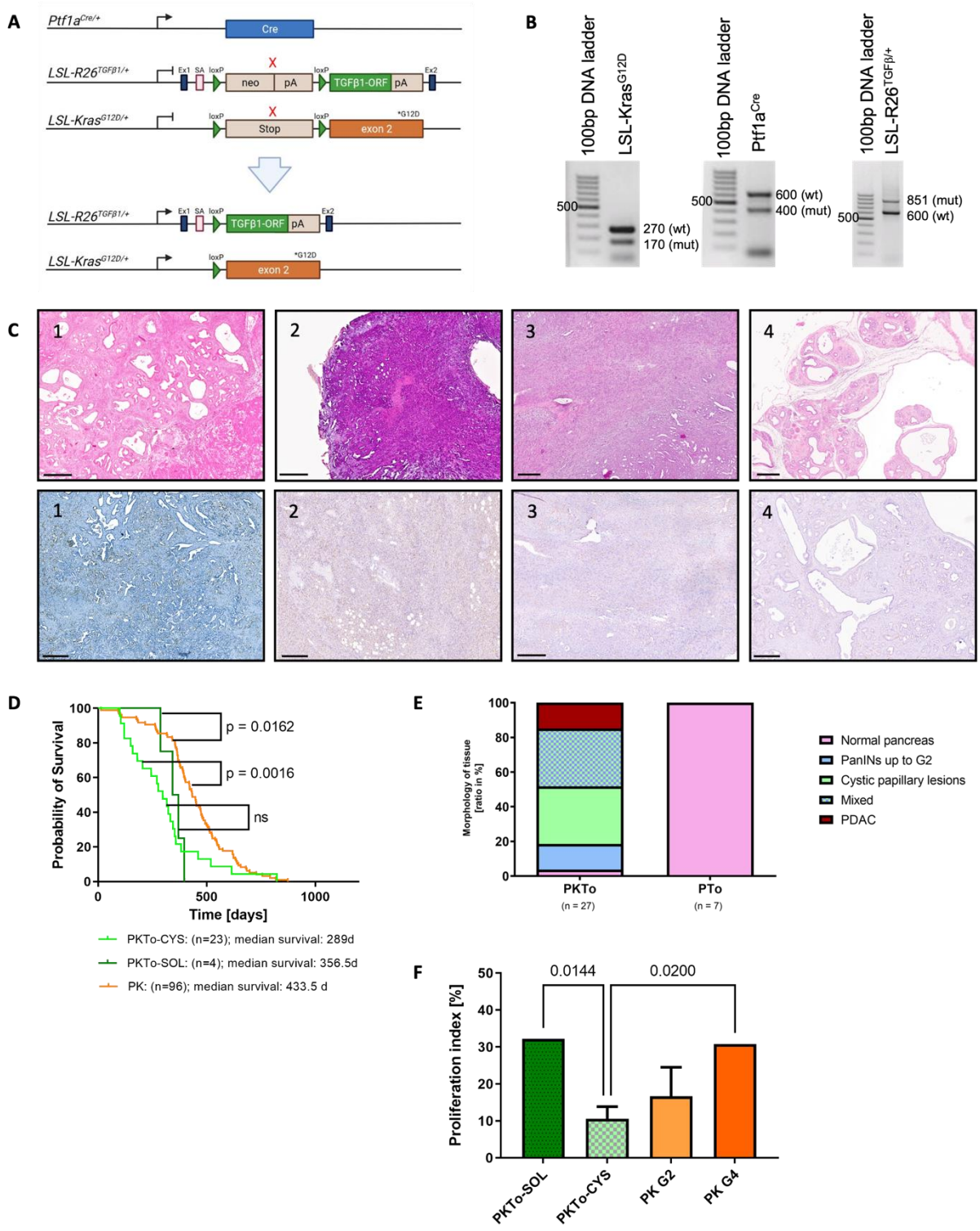

Figure 1: *Tgfβ1* overexpression influences PDAC progression and leads to distinct histopathological phenotypes

(A) From top to bottom, diagrams of: the *Rosa26* locus with LSL-silenced *Tgfβ1* expression cassette; the *Rosa26* locus after Cre-induced deletion of the *LSL* cassette with activated *Tgfβ1*expression;

Genetic strategy used to activate oncogenic *Kras*^{G12D} with the *Cre-LoxP* recombination system under control of the pancreas specific promotor *Ptf1a*; pA: polyadenylation sequence; SA: splice acceptor. Ex: exon

(B) Genotype confirmation of PKTo mice: PCR results are shown for LSL-Kras^{G12D} (mut: 170bp; wt: 270bp); Ptf1a^{Cre} (mut: 400bp; wt: 600bp) and LSL-R26$^{TGF\beta/+}$ (mut: 851bp; wt: 600bp); mut: mutated; wt: wild type

(C) Representative microscopic images (H.E. and Ki67) of pancreata from PK with (1) differentiated and (2) undifferentiated phenotype, (3) PKTo-SOL and (4) PKTo-CYS mice; Scale bar 300µm.

(D) Kaplan-Meier survival analysis of PKTo-SOL, PKTo-CYS and PK mice. The p-value was calculated using Mantel-Cox-test.

(E) Overview of the morphology of the pancreata of PKTo-TM (n=27) and PTo (n=7) mice. Bar graph shows the percentage of mice with their most prominent tissue type.

(F) Proliferation index of PKTo-SOL mice with PDAC (n=2) and PKTo-CYS mice with cystic papillary lesions (n=4) compared to PK mice with differentiated G2 (n=3) or undifferentiated G4 (n=2) PDAC. Bar graph shows the percentage of cells stained positive for Ki67 as proliferative marker. Data are shown as mean ± SD of 10 fields of view for 1 representative slide per mouse, only significant p-values are shown calculated by one-way ANOVA.

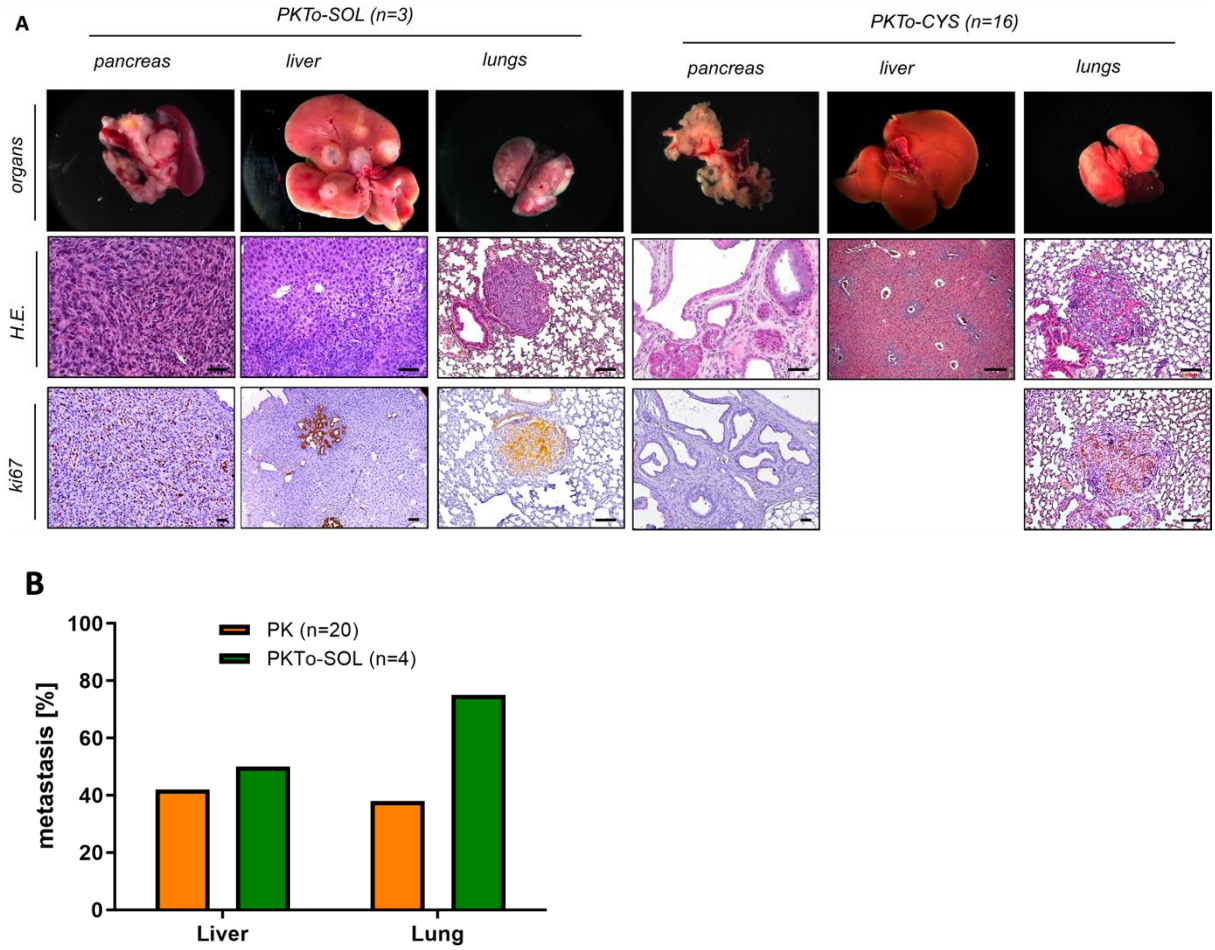

Figure 2: The solid PKTo PDAC subtype is highly metastatic compared to the cystic PKTo subtype

(A) Representative macroscopic (brightfield) and microscopic images (H.E., Ki67 and Ck19 staining) of pancreata from PKTo mice. Left: PKTo mice displaying an invasive carcinoma, liver and lung metastasis; Right: PKTo mice showing cystic papillary lesions and no metastasis; Scale bar 100µm

(B) Quantification of liver and lung metastasis of PKTo-TM (n=4) compared to PK mice (n=20) with histologically confirmed PDAC. Bar graph shows the percentage of mice with liver and lung metastasis. Data of PK mice were derived from (Eser et al., 2013).

5.2 Pancreas-specific *Tgfβ1* overexpression alone does not lead to PDAC formation

In addition, to analyse the influence of *Tgfβ1* in the context of *Kras*^{G12D} PDAC initiation, we investigated the effects of *Tgfβ1* overexpression alone. Therefore, PTo mice were analysed on two different time points (three and twelve months). As a result, pancreas-specific *Tgfβ1* overexpression alone did not display PDAC formation or other histopathological changes in the pancreas (Figure 3A and B). Next, PTo mice were aged and analysed for survival. The median survival of PTo animals was 531.5 days (see Figure 3C).

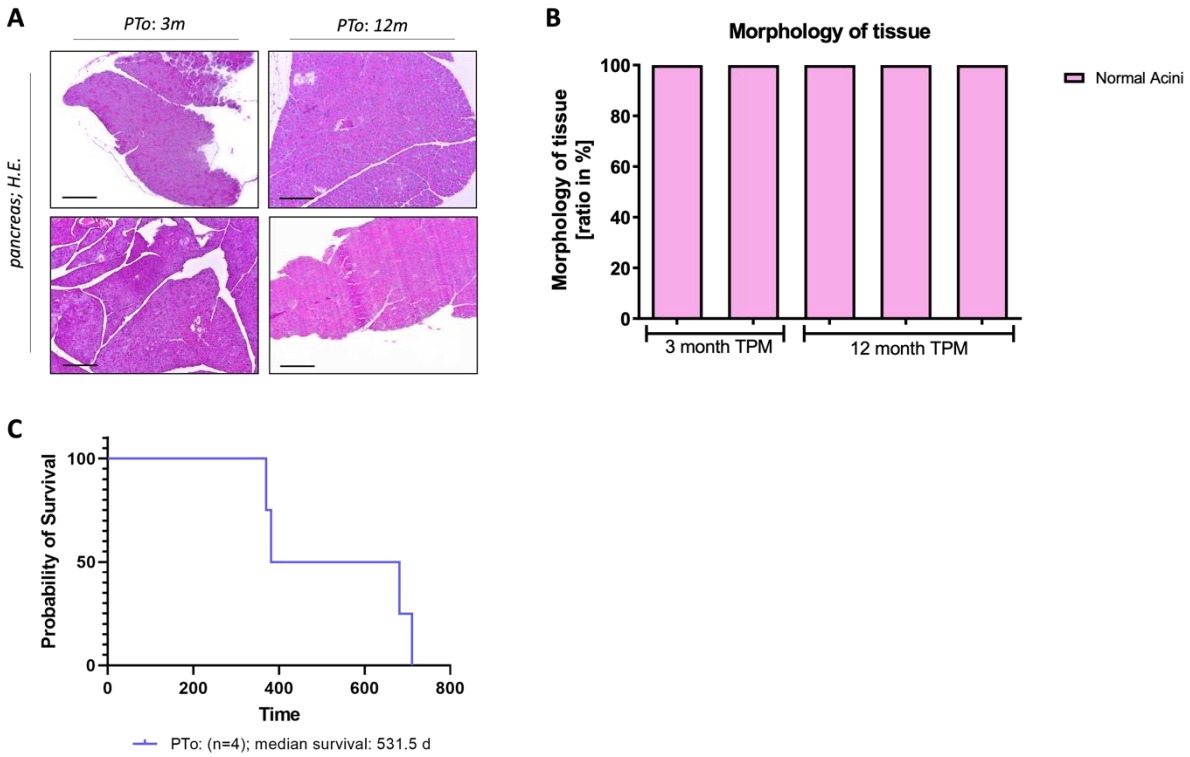

Figure 3: PTo mice do not display PDAC formation

(A) Representative microscopic images (H.E. staining) of pancreatic tissue from PTo (age from left to right; respectively: three and twelve months). Scale bar 300µm.

(B) Analysis of pancreatic tissue images (H.E. staining) of PTo mice. Percentage share of different tissue types of the pancreas in three (n=2), and twelve (n=3) months old PTo mice (1 representative slide per mouse; each bar represents one mouse).

(C) Kaplan-Meier survival analysis of PTo mice.

5.3 Cystic phenotype develops over time as PKTo mice mature

In the next analysis, we investigated the histopathological development of PKTo pancreatic tissue over a time course of twelve months, since the median overall survival of PKTo mice was 307.5 days. For this purpose, three PKTo mice per timepoint were sacrificed at the age of three, six, nine and twelve months. The H.E.-stained pancreatic tissue (displayed in Figure 4A) was classified into normal acini, stroma, cystic papillary lesions, PanINs or PDAC and the percentage share of the area of different tissue types was calculated for one representative slide per mouse as shown in Figure 4B. If present, PanIN lesions were classified, counted and their density in the tissue was calculated.

None of the PKTo timepoint mice (PKTo-TPM) developed an invasive carcinoma. Three months PKTo-TPM still showed areas of normal intact acini, which decreased in nine- and twelve-months old mice. PanIN precursor lesions were limited to PanIN-1A, -1B and -2, whereas PanIN-3 lesions were not present for all time points. The overall density of PanIN lesions was comparable for mice of all time points as displayed in Figure 4C. Of note, some of the nine- and twelve-months old mice displayed pancreata consisting of cystic papillary lesions only, which was not the case in three- and six months old mice. This explains the much higher standard deviation of PanIN density in older mice. The formation of cystic papillary lesions accelerated over time as seen in Figure 4B.

In conclusion, time-point analysis of mice with constitutively active *Tgfβ1* overexpression showed formation of cystic papillary lesions at a very early stage. The quantity of these cystic lesions increases and shows a continuous progression over time. Very little to no functional acini remain, yet no PDAC developed in these mice.

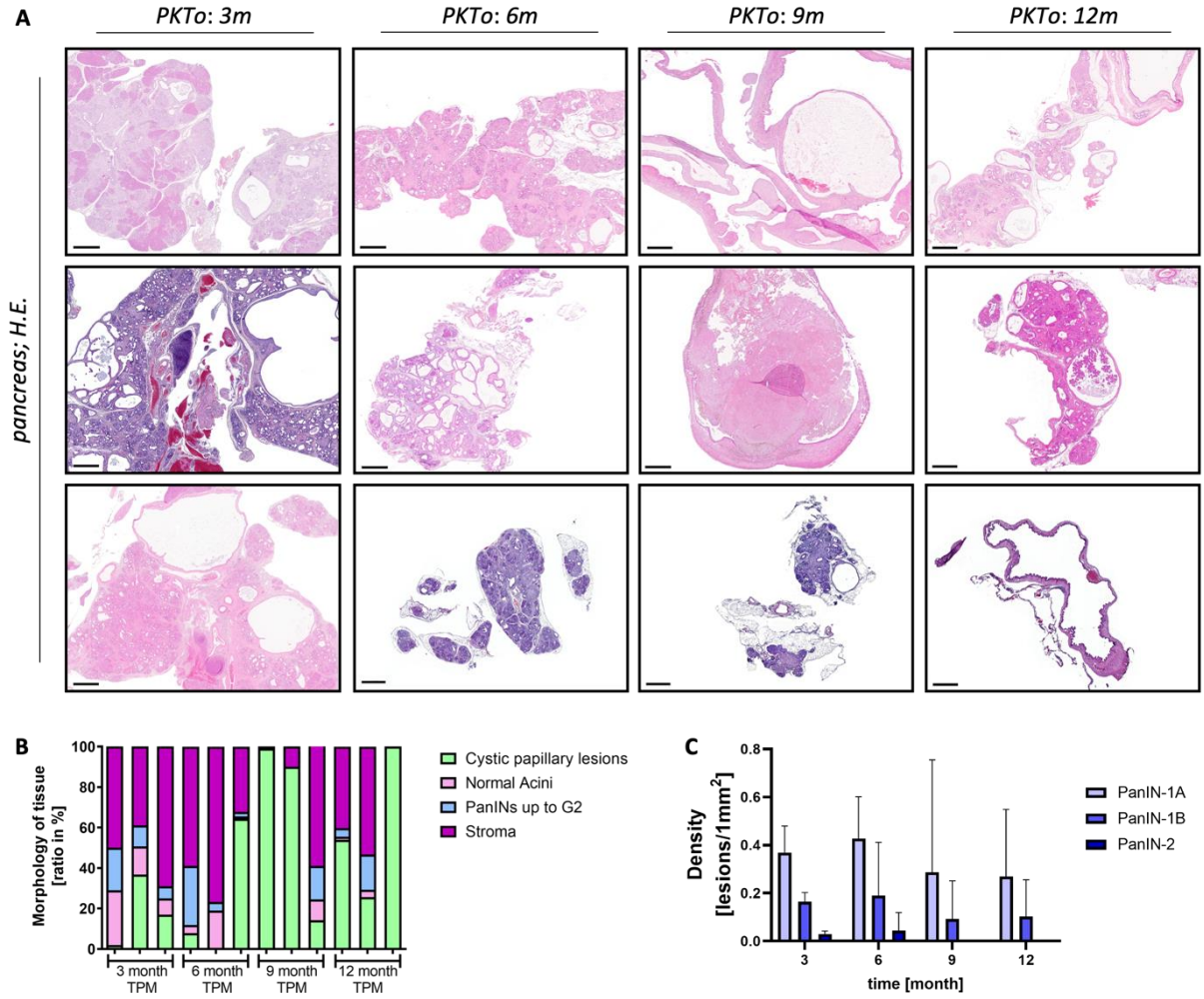

Figure 4: Time-point analysis of PKTo mice reveales a continuous progression of cystic papillary lesions

(A) Representative microscopic images (H.E. staining) of pancreatic tissue from PKTo-TPM (age from left to right; respectively: three, six, nine and twelve months; three different mice per timepoint). Scale bar 700µm.

(B) Analysis of pancreatic tissue images (H.E. staining) of PKTo-TPM; Percentage share of different tissue types of the pancreas in three, six, nine and twelve months old PKTo mice (n = 3 mice per timepoint; 1 representative slide per mouse).

(C) Quantification of PanIN lesions in three, six, nine and twelve months old PKTo mice (n = 3 mice per timepoint; 1 representative slide per mouse); mixed-effect analysis showed no significant differences.

5.4 Histopathological phenotype of PKTo mice *in vivo* matched morphological phenotype of *in vitro* cell cultures

We isolated three cell lines from the pancreatic tissue of PKTo mice. Two of these originated from PKTo-SOL mice and only one cell line could be cultivated from PKTo-CYS mice. Establishing cell lines from the PKTo-CYS subtype appeared to be far more challenging than from the PKTo-SOL subtype, as their pancreatic lesions were non-invasive and proliferated less as described in 5.1.

Cell lines from mice with more benign, cystic phenotype (PKTo-CYS) had a mesenchymal morphology with typical spike-like extensions and rare cell-cell-adhesions, whereas cell cultures from invasive PDAC (PKTo-SOL) showed an epithelial morphology with roundly shaped and interconnected cells as depicted in Figure 5A. Cells from PK mice were chosen in respect of their phenotype accordingly and divided in two subgroups: mesenchymal PK-cell lines (PK-C1) and epithelial PK-cell lines (PK-C2). These cell lines were comprehensively characterized as published elsewhere (Mueller et al., 2018).

Successful recombination was shown for *Kras.* One PKTo-SOL cell line showed loss of heterozygosity as well as all PK-C2 cell lines. The presence of mutant Tgfβ1 was also confirmed in PKTo cell lines as depicted in Figure 5B.

Furthermore, our lab previously generated cell lines from PDAC in PKT-HOM mice. A homozygous knock-out of the *Tgfbr2* is present in addition to oncogenic $Kras^{G12D}$, thereby abrogating tumour cell intrinsic Tgfβ downstream signalling. Cell lines from pancreata of PKT-HOM mice were additionally evaluated for the possibility to compare acquired PKTo tumour cells on a molecular level. One PKTo-HOM cell line showed an epithelial, the other a mesenchymal cell type.

The proliferation of all different cell lines was analysed with viability assays, using MTT and clonogenic assays.

Clonogenic assays were conducted with a seeding concentration of 2000 cells per well and cultivated for six days. The formation of colonies in PKTo-CYS cell lines was impaired and they displayed very diffuse, poorly demarcated colonies as shown in Figure 5C. This was not the case for PK-C1 cells, their morphological control group. All other cell lines presented with defined colonies and there was no significant difference in numbers of colony formation observed (Figure 5D).

MTT assays were conducted with a seeding concentration of 500 cells per 100 µL and are depicted in Figure 5E. The growth speed of PKTo-SOL cell lines was similar compared to PK cell lines, regardless of their morphology. No significant differences were detected. On the contrary, PKTo-CYS cell lines grew significantly slower compared to all other cell lines.

In summary, PKTo-CYS cell lines are less viable and proliferate slower than their PKTo-SOL counterpart and control groups, respectively. This data is consistent with the histopathological evaluation of PKTo-CYS tumours and their non-invasive behaviour.

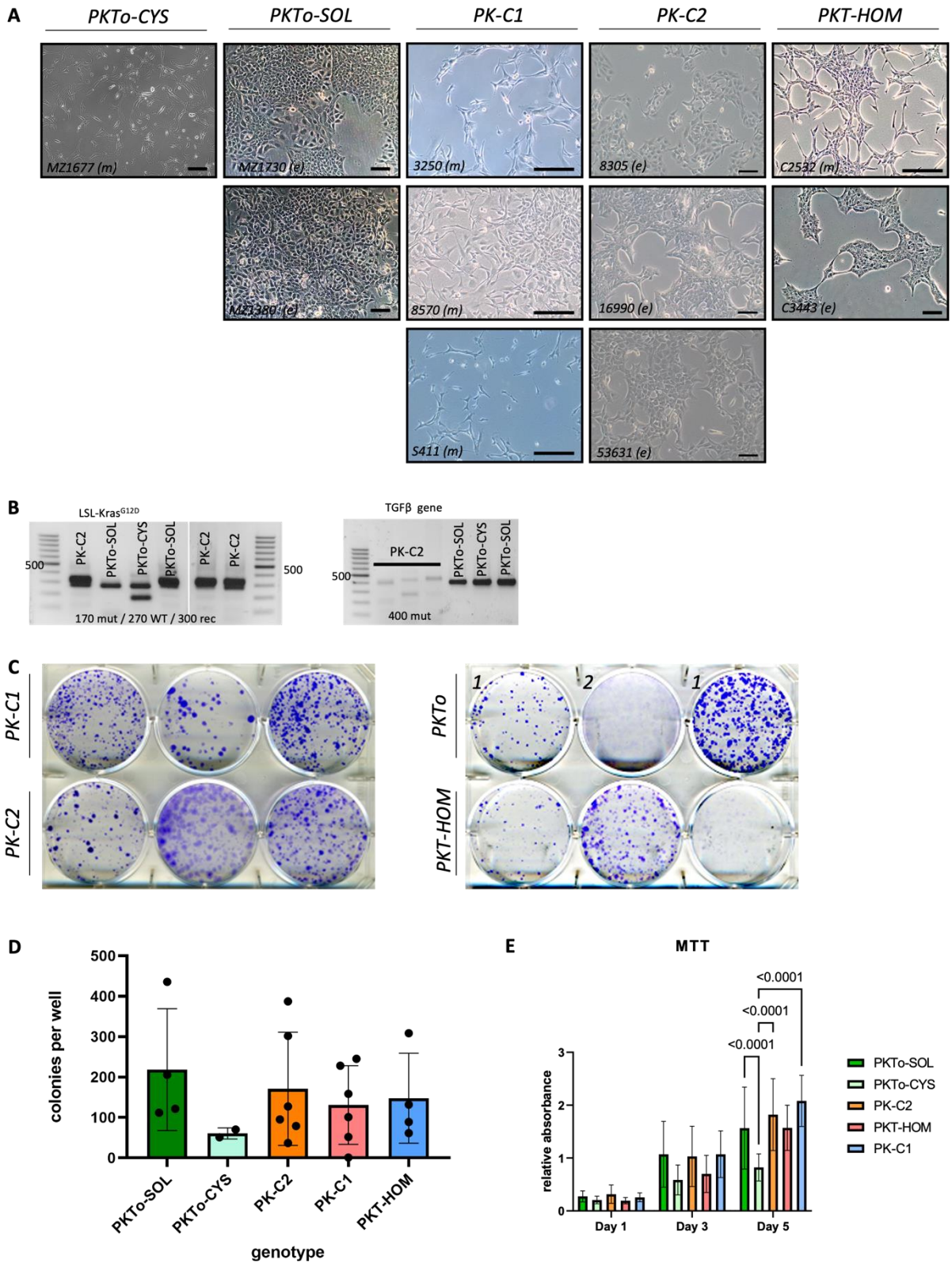

Figure 5: Cystic and solid PKTo cell cultures show distinct morphological phenotypes and no difference in proliferation

(A) Representative pictures of PKTo, PK and PKT cell lines showing either epithelial (e) or mesenchymal (m) cell type; Scale bar 100µm.

(B) Genotype confirmation of PKTo cell lines: PCR results are shown for LSL-Kras^{G12D} (mut: 170bp; wt: 270bp); and LSL-R26$^{TGF\beta/+}$ (mut: 400bp); mut: mutated; wt: wild type

(C) Representative images of clonogenic assay experiments of PKTo (1 -SOL; 2 -CYS), PK-C1, PK-C2 and PKT-HOM cell lines.

(D) Clonogenic assays of PKTo -SOL (n=2), -CYS (n=1), PK-C1 (n=3), PK-C2 (n=3) and PKT-HOM (n=2) cell lines. Plot depicts quantification of colonies per well. Data of n=2 experiments with 3 replicates are shown. 2way ANOVA showed no significant differences between groups.

(E) MTT assays of PKTo-, PK and PKT cell lines were evaluated on day one, day three and day five after seeding and compared to each other. Results are grouped according to genotype. Data is normalized to day zero. Data are shown as mean ± SD; n = 3 replicates; p-values are calculated with one-way ANOVA, only significant p-values are shown.

5.5 Induction of *Tgfβ1* in FKTo mice leads to cystic papillary lesions of the pancreas

In the previous analyses, we investigated the influence of *Tgfβ1* overexpression on PDAC initiation and observed that most PKTo mice developed cystic papillary lesions. Therefore, we analysed next the time-specific effects of *Tgfβ1* overexpression using a dual-recombinase mouse model. FKTo mice constitutively express mutant *Kras* under the pancreas-specific *Pdx1-Flp* recombinase and allowed us to activate *Tgfβ1* overexpression in the pancreas at specific timepoints due to the tamoxifen-inducible *FSF-R26*$^{CAG\text{-}CreERT2/+}$ allele (Schönhuber et al., 2014) as depicted in Figure 6A. Consequently, *Kras*^{G12D} is active from the beginning, while *Tgfβ1* is only active after tamoxifen treatment of these mice.

FKTo mice were treated with a mixture of tamoxifen chow and i.p. injections for three weeks (as described in 4.2.1.3 Tamoxifen treatment of mice) either at three months age, then sacrificed at nine months age, or treated at six months age and sacrificed, when mice became moribund (see Figure 6B).

The FKTo control group received i.p. injections with peanut oil suspension medium only and no tamoxifen was applied. Hence, *Tgfβ1* overexpression was not induced, but we could exclude changes of pancreatic tissue or mouse wellbeing due to the invasive treatment procedure. Mutant *Kras* was active in FKTo control mice, similar to the PK control group.

FKTo mice treated with tamoxifen at six months age (FKTo-6mTAM) had a median survival of 609 days, whereas in mice treated with placebo (FKTo-6mplac) it was 489 days. With a small sample size of n = 3 in both groups, this difference was not statistically significant as shown in Figure 6C (p-value = 0.2769 calculated with Mantel-Cox test).

The mean weight of FKTo-6mTAM pancreata was 0.87 g (±0.27) and 1.46 g (±0.56) for pancreata of FKTo-6mplac mice as shown in Figure 6D. This difference is not statistically significant (p-value = 0.5764, calculated with one-way ANOVA)

H.E.-stained pancreatic tissue (displayed in Figure 6E) was evaluated similar to PKTo-TPM mice as described above. The percentage share of the area of different tissue types (normal acini, stroma, cystic papillary lesions, PanINs, PDAC or necrosis) was calculated for one representative slide per mouse for three mice per timepoint as shown in Figure 6F. FKTo mice treated with tamoxifen at three months age (FKTo-3mTAM) presented a completely healthy pancreatic tissue at the age of nine months, whereas mice treated with placebo (FKTo-3mplac) already showed beginnings of low grade PanIN lesions, as shown in Figure 6F.

FKTo-6mTAM with activated *Tgfβ1* developed a histopathological change of the pancreas towards cystic papillary lesions and fibrotic tissue and showed no development towards invasive PDAC. In contrast, FKTo-6mplac mice presented with PDAC and metastasis in liver and lungs (data not shown).

In conclusion, the time-dependent activation of *Tgfβ1* at the age of three months supressed the formation of low-grade lesions and activation at six months lead to cystic papillary lesions and fibrosis instead of development into PDAC. This suggests a tumor suppressive role of *Tgfβ1.*

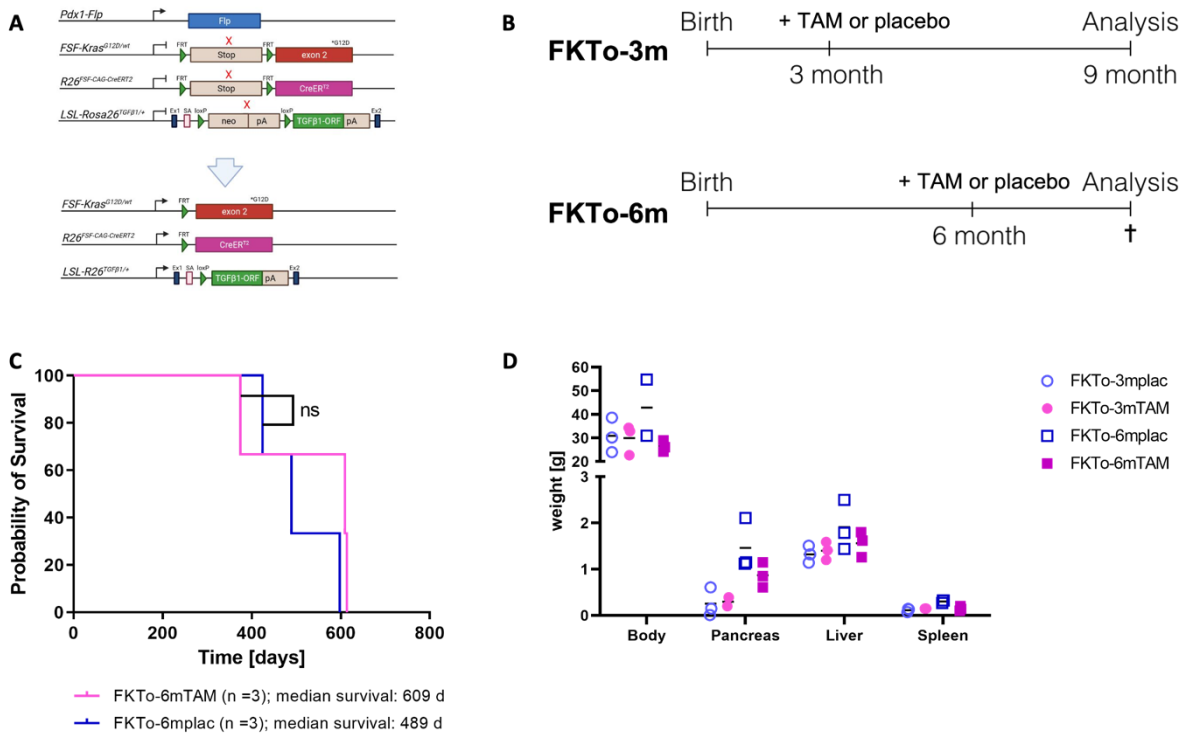

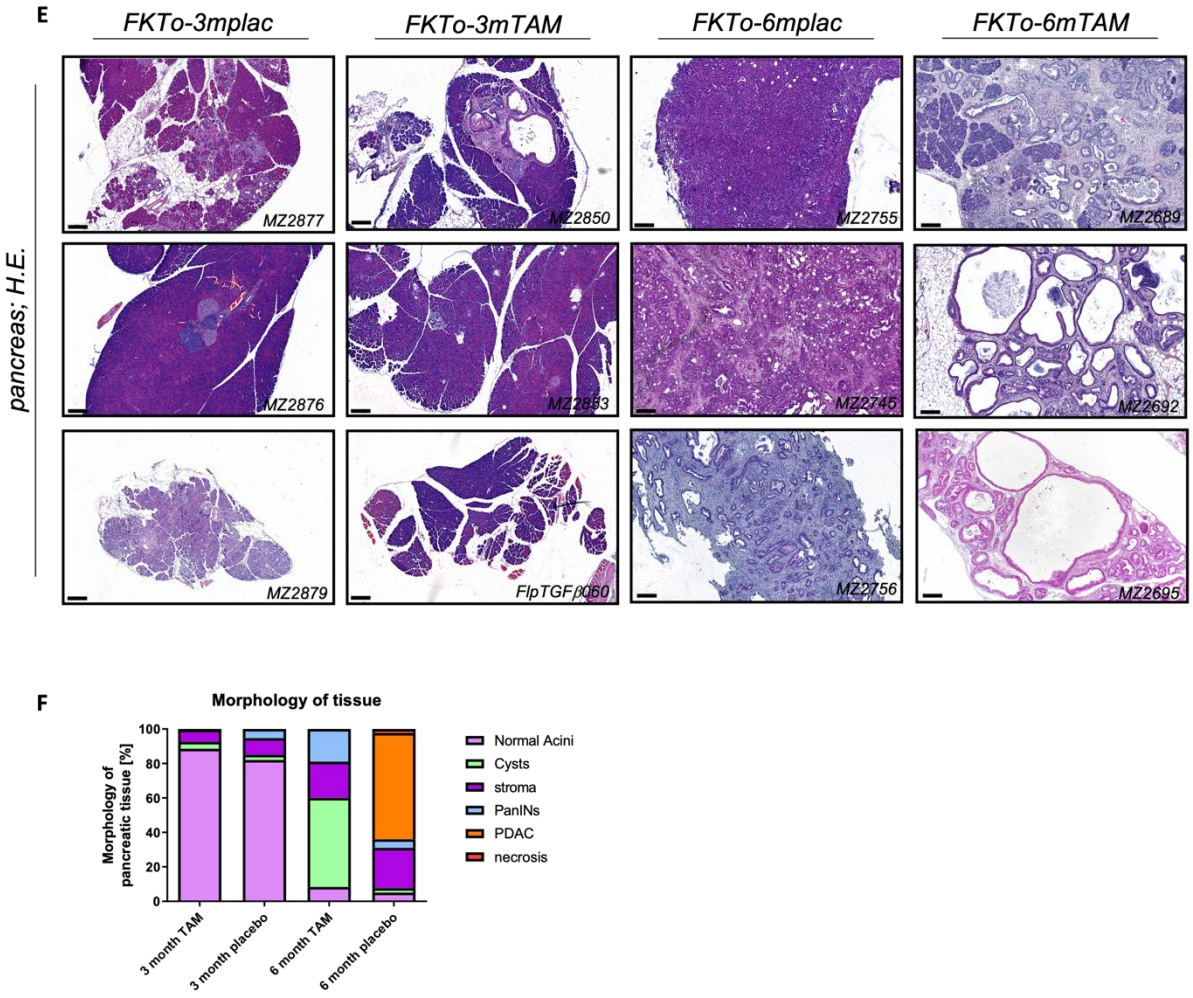

Figure 6: Time-dependent *Tgfβ1* overexpression leads to development of cystic lesions and prevents PDAC formation

(A) Genetic strategy to activate *Tgfβ1* by time-specific tamoxifen-mediated *CreER^{T2}* recombination using a dual recombinase system. *Kras^{G12D}*, activated by *Pdx1-Flp*, induces PanIN lesions. *CreER^{T2}* is activated by TAM administration and activates LSL-silenced *Tgfβ1.*

(B) Schematic treatment protocol of FKTo and control mice

(C) Kaplan-Meier survival analysis of FKT-6mTAM and FKT-6mplac. The p-value was calculated with Mantel-Cox-test and no significant differences were detected between groups.

(D) Weight of FKTo mice and their organs. Data are shown as mean of n = 3 mice per group. The p-value was calculated with one-way ANOVA and no significant differences were detected.

(E) Representative microscopic images (H.E. staining) of pancreata from TAM-treated FKTo (n = 3) and placebo-treated FKTo (n= 3) mice; Scale bar 200µm

(F) Percentage share of different tissue types of the pancreas of FKTo mice (n = 3 mice per group, 1 representative slide per mouse).

6 Discussion and Outlook

Similar to other cancer types, the stepwise progression from precursor lesions to an invasive carcinoma became an established model for the development of PDAC (Distler et al., 2014). Oncogenic *KRAS* is a very early mutation and most frequent in human PDAC, which lead to GEMM, mirroring human PDAC progression with $Kras^{G12D}$-driven genetic strategies (Guerra & Barbacid, 2013; Hingorani et al., 2003). Further genetic alterations progress the dysplasia of PanIN lesions into invasive carcinomas. SMAD4 inactivation as TGFβ downstream effector was shown to be one of them (Jones et al., 2008). On the contrary, active TGFβ was also shown to facilitate cell invasion, migration and metastasis (David & Massague, 2018). Since the role of TGFβ in cancer is a controversial topic, this projects aim was to shed light onto the dual function of TGFβ by analysis of *Tgfβ1* overexpression in a $Kras^{G12D}$-driven PDAC model.

Tgfβ1 overexpression in the presence of oncogenic *Kras* had diverging effects on pancreatic tissue in a time-dependant matter. Histopathological changes towards cystic papillary lesions occurred in models with constitutively overexpressed *Tgfβ1* and furthermore, delayed overexpression led to dismantling of preformed PanIN lesions and repression of PDAC development. However, eventually emerging cancer in 14.8 % of cases showed an aggressive, dedifferentiated primary tumour and accelerated metastasis rates highlighting the time- and context-depending dual role in cancer progression and suggesting distinct evolutionary routes of tumorigenesis into two phenotypes. It is important to perform further research to investigate and ultimately understand the genetic basis of these two phenotypes.

6.1 Precursor switch towards cystic lesions

Cystic lesions of the pancreas are quite frequent, and a rising number of patients are diagnosed with asymptomatic pancreatic cystic lesions during the last decade due to improved and sensitive imaging. Most of these lesions are benign and their occurrence is strongly correlated with age. Various studies have shown incidental cystic changes of pancreata with a range from 2 to 25% of screened patients, depending on their circumstances (e.g. screening due to pancreas-related or not-pancreas-related symptoms). Neoplastic changes are seldom, but possible, and accurate prediction which cysts develop into invasive carcinomas are challenging (Matthaei et al., 2011).

The most common neoplastic precursor lesions are PanINs, followed by cystic lesions as IPMNs and MCNs (see also 3.2). Both cystic type lesions display few similar genetic alterations, when compared to PanIN lesions, but differ in terms of frequency and

timepoint. For example, *KRAS* activating mutations incidence is lower in IPMNs and MCNs and *SMAD* mutations tend to be present in invasive lesions, whereas they appear already in PanIN-2 or -3 lesions. Apart from these few genetic markers, cystic lesions are far less researched than PanINs, mainly because of their low prevalence and the lack of an accurate mouse model (Distler et al., 2014; Matthaei et al., 2011). First results for the development of a reliable mouse model were made in 2007 by Schmid and colleagues, as they crossed mice harbouring oncogenic *Kras* with *Tgfα* overexpression and discovered the formation of cystic papillary lesions resembling IPMNs (Siveke et al., 2007).

In our work, *Tgfβ1*-overexpression also lead to the development of cystic papillary lesions. Mice at an early age presented with a coexistence of low-grade PanIN lesions and cystic lesions, whereas older mice mostly displayed exclusively cystic lesions.

Even after development of few PanIN lesions due to active *Kras*, the activation of *Tgfβ1* in FKTo mice at the age of 6 months repressed PDAC progression and an alternative route towards cystic papillary lesions developed instead. Significantly enhanced TGFβ signalling was also described in the analysis of the TGFα mouse model (Siveke et al., 2007).

On the contrary, *Kras* mouse models with *Smad4* haploinsufficiency induced development of cystic lesions resembling MCNs. Interestingly, loss of both *Smad4* alleles lead to IPMN-like lesions, suggesting a dependency on gene dosage. Either way, *Smad4* loss seemed to be a steppingstone for the development of cystic lesions but all pancreata also yielded PanIN lesions at the same time (Izeradjene et al., 2007; Kojima et al., 2007).

A working model was proposed which describes two different routes of pancreatic ductal epithelium, leading to invasive ductal adenocarcinoma in the end. As precursor lesions display a similar mutation profile, it is suggested that early LOH of *SMAD4* leads to MCNs, whereas genetic alterations of *p53* or *p16* first lead to advanced PanINs and *SMAD4* LOH takes place in already more advanced stages (Kojima et al., 2007).

These findings seem to contradict our data as abrogated TGFβ signalling due to defects in SMAD4 signalling lead to development of cystic lesions. Therefore, it is important to investigate the SMAD4 status in our mouse model on genetic and protein level. Furthermore, the distinction of these cystic papillary lesions via immunostainings was not done in this work yet and the exact determination, whether these developing lesions are IPMNs or MCNs should be subject to further research.

Our mouse model harbouring oncogenic *Kras* and *Tgfβ1* overexpression may be a possibility to generate mouse models, mirroring the formation of cystic lesions of the pancreas. Moreover, the further understanding of TGFβ signalling in PDAC cells and analysis of its underlying pathways may present a useful tool to identify risk patients for cystic pancreatic tumour entities in the future.

The difficulties in cell culturing are disadvantageous –from 23 PKTo mice pancreata only one cell line could be cultivated. The usage of organoids could be explored as an alternative for this model (Beato et al., 2021).

6.2 Decreased survival time

The survival time of PKTo mice was reduced compared to the PK control group, even though the majority did not develop PDACs. We assume the reason is a developing exocrine pancreas insufficiency which is accompanied by chronic abdominal pain, maldigestion and weight loss (Tyler Stevens, 2020), conditions in which mice are being sacrificed. Pancreas insufficiency is also observed in cystic fibrosis patients, a disease extensively linked to elevated TGFβ levels (Kramer & Clancy, 2018). To investigate the decreased survival time we suggest laboratory blood work, functional test of the pancreas, if feasible, and abdominal imaging of the mice to evaluate the degeneration of the pancreas over time and confirm exocrine pancreas insufficiency.

6.3 Role of TGFβ in PDAC progression

Tgfβ1 overexpression was shown to have a diverse effect on pancreatic tissue harbouring oncogenic *Kras*. The pancreata of these mice performed a morphological change towards cystic papillary lesions, instead of classic PDAC initiation. Even after development of few PanIN lesions due to active *Kras*, the activation of *Tgfβ1* at the age of 6 months repressed PDAC progression. The two distinct routes into either benign or more aggressive tumour types, which were detected in this work, have already been observed in various other tumour models e.g. in skin carcinomas, colon cancer or breast cancer (Padua & Massague, 2009). In general, TGFβ is viewed as tumour suppressor in context of premalignant cells. This is the case in our PKTo model, where histopathological analysis of mice with constitutively active *Tgfβ1* is consistent with tumour suppressive functions. It was shown, that intact SMAD signalling leads to apoptosis in premalignant *Kras* driven PDAC progenitors (Bardeesy et al., 2006). Disruptions of the canonical TGFβ pathway, in PDAC often implemented through abolition of SMAD4, is suspected to be the cause for acquisition of tumour promoting effects of TGFβ (David & Massague, 2018). Therefore, a further understanding of TGFβ downstream signalling is needed in the PKTo model and suspectedly abrogated SMAD4 signalling needs to be investigated. In the time-dependent mouse model with a dual recombinase system, early induction of *Tgfβ1* lead to normal pancreatic tissue, whereas later induction at the age of 6 months lead to cystic papillary lesions instead of PanIN formation and PDAC. We assume that with tamoxifen treatment

at six months age, *Tgfβ1* overexpression hit low-grade PanIN lesions in a premalignant context. Due to an intact downstream pathway, tumour suppressive functions were activated and precursor lesions became apoptotic eventually. The mechanics through altered regulation of KLF5 and SOX4 are described as “lethal EMT” (David et al., 2016). Consequently, we should inquire KLF5 and SOX4 status of early treated FKTo mice. Secondly, a new experimental setup with tamoxifen treatment of FKTo mice at a later time point after eventual loss of canonical signalling should be done. Since the median survival was 609 days treatment in twelve or 15 months old mice could be tested.

Furthermore, mice with sole pancreas-specific overexpression of *Tgfβ1* did not show any signs of tumour development. This was for example also observed in *Ptf1a*$^{Cre/+}$*; Tgfbr2*$^{lox/lox}$ mice, where the pancreas appeared to be normal (Ijichi et al., 2006). Therefore, neither TGFβ overexpression, nor blockade of TGFβ signalling are sufficient to initiate PDAC and additional mutations or triggers for example oncogene *Kras* are required for this process.

Three major *KRAS* signalling pathways are believed to be essential in PDAC: The first identified *MAPK* pathway as well as *PI3K-PDK1-AKT* and the Ral guanine nucleotide exchange factor pathway (Collisson et al., 2012; Eser et al., 2013; Lim et al., 2005). Both, complementary and antagonistic effects of the interaction between the RAS downstream pathways and TGFβ have been observed.

In the MAPK-pathway, GTP-bound RAS recruits Raf to the plasma membrane and activates it, which leads to a phosphorylation and thus activation cascade of MEK1/2 and ERK1/2. ERK has many downstream targets, which are responsible for cell cycle regulation such as Cyclin D or MYC (Malumbres & Barbacid, 2003). Especially ERK, is a shared target of RAS and TGFβ. Up to date activating as well as inhibitory cross talks between ERK and TGFβ were discovered. ERK has been shown to inhibit SMAD signalling by disabling SMAD activity (e.g. through phosphorylation of SMAD1, 2 or 3), reducing TGFβRI density on the cells surface or negatively interacting with its transcription factors. Other studies indicated a positive effect on the SMAD pathway by enhanced ERK-MAPK gene transcription (Mu, Gudey, & Landstrom, 2012). TGFβ-induced ERK activation was detected in various different cell types like epithelial cells, colon cancer cells or fibroblasts. In vitro studies showed a rise of ERK phosphorylation through TGFβ-treatment, both after 5-10 min and after multiple hours, suggesting the existence of direct as well as indirect interactions (Luo, 2017; Mulder & Morris, 1992; Simeone et al., 2001).

AKT is another important KRAS downstream target and deregulated in many human cancers - foremost because of its anti-apoptotic effects, but also other cellular processes, like proliferation or cytoskeletal rearrangements (Downward, 2004; Revathidevi & Munirajan, 2019). Combination with TGFβ especially facilitates EMT. TGFβ activates

PI3K, which leads to AKT phosphorylation, and therefore activation. An important AKT downstream effector is mTOR, which seems to play a critical role in TGFβ-induced EMT due to its ability to influence cell growth, proliferation and motility (Lamouille & Derynck, 2007). Furthermore, AKT activates EMT transcription factors (EMT-TF) through direct phosphorylation (e.g. Twist1) or indirect loops (e.g. inactivating GSK3β, a powerful SNAI1 inhibitor). Additionally, AKT and TGFβ also have antagonistic effects, since AKT inhibits SMAD3-mediated transcription. This may be a possibility to suppress TGFβ-mediated growth arrest (Luo, 2017; Zhang, 2009, 2017).

These cross talks of TGFβ and KRAS downstream effectors may be an explanation for a small quantity of PKTo mice developing aggressive PDAC. In one of the two isolated PKTo-SOL cell lines a loss of heterozygosity of the *Kras* allele was observed. It was shown that increased gene dosage of $Kras^{G12D}$ is connected to increased metastatic potential and thus drives early progression and metastasis (Mueller et al., 2018). Furthermore PKTo-SOL histopathological proliferation parameter as well as proliferation evaluation of cell lines showed similar behaviour to undifferentiated PK tumours. Consequently, ERK and AKT activity needs to be further evaluated in the PKTo mouse model on RNA and protein level. Up until now protein quantification via westernblot remained inconclusive (data not shown).

In conclusion, pancreatic tissue of PKTo mice mostly showed a more benign phenotype with low-grade PanINs and cystic papillary lesions, consistent with the tumour-suppressive functions of TGFβ. However, eventually emerging cancer in 14.8 % of cases were more aggressive, presenting with a primary tumour harbouring a dedifferentiated, invasive cell type and leading to fast metastasis implying a tumour promoting role. Therefore, it is important to perform genomic analysis to understand the genetic basis of these two phenotypes.

6.4 Conclusion and Outlook

In this doctoral thesis, a novel *Tgfβ1* overexpression PDAC mouse model was systematically characterized to understand the role of *Tgfβ1* in tumour initiation and progression. The histological characterization showed a shift from well-known PanIN lesions towards cystic papillary lesions. opening the possibility of creating a new mouse model for these rarer precursor lesions. Also, these types of lesions are associated with a more benign progression and do not develop invasive carcinomas. The identification of the exact pathology of these cystic lesions through immunostainings should be done in the future to determine, whether these are MCN or IPMN. This distinction seems to be important since they showed different types of mutation or change in the order of occurring mutations in previous publications. Furthermore, a medical evaluation of mice with TGFβ1-overexpression and cystic phenotype should be done to evaluate the cause of lowered overall survival of these mice. We suspect the degeneration of the pancreas with resulting exocrine pancreas insufficiency as the cause of the worsening condition of these mice.

On the other hand, eventually emerging tumours in this mouse model seemed to be aggressive and showed a higher metastasis rate, comparable to undifferentiated G4 mPDACs. To identify the trajectories leading to benign or aggressive morphology, we need to evaluate the downstream effects of TGFβ1 overexpression with genomic analysis of documented key regulators like SMAD4, ERK, AKT, KLF5 and SOX4. Problems of cultivating cell lines can be faced by establishing organoids from PKTo-CYS mice. Furthermore, cell lines established from FKTo mice, which were not treated with tamoxifen in vivo can be treated in vitro to observe the effect of TGFβ1 in context of malignant cells. An evaluation of mutational gains in these mice is necessary to understand the mechanisms behind TGFβ1 activation.

In summary, tumour suppressive effects of TGFβ1 in context of premalignant progenitors were validated in this thesis. Still, the molecular mechanisms of TGFβ in tumour initiation, progression and metastasis have to be unravelled in further research.

6.4.1 The contribution of the microenvironment

Research on underlying pathways and genetic alteration of human cancer cells enabled the production of new targeted therapies, seemingly grasping the origin of cancer. The explanatory concept of a primary cancer cell and its underlying cancer driver mutations was challenged as the success of novel anti-cancer drugs, targeting specific gene sites, was often dependent on the anatomical tissue type; off-label use in different tissues exhibiting the same genetic alterations did not prove to be superior. This leads to the conclusion, that oncogenic drivers and pathways are still very tissue-specific and have to

be evaluated in context of the anatomical site and its micro- and macroenvironment (Schneider et al., 2017). Earlier on, underlying chronic inflammatory diseases were already described as risk factor for eventually emerging cancer types; approximately 15% of human cancers can be back traced to such conditions like chronic pancreatitis, gastritis, cirrhosis or Colitis/Crohns disease (Coussens & Werb, 2002), reinforcing the role of tissue microenvironment in light of cancer development and progression.

Compared to other epithelial tumours, pancreatic cancer has a very prominent stromal reaction, consisting of extracellular matrix (ECM) and stromal cells like cancer-associated fibroblasts (CAF), endothelial cells and immune cells. This dense desmoplastic stroma leads to drug resistance and support a tumour-favourable environment through immune cell evasion, enhanced tumour growth and metastasis (Murakami et al., 2019). It was shown, that TGFβ1 is able to induce desmoplasia in pancreatic tissue (Lohr et al., 2001) through various mechanisms, for example activation of CAFs (Sun et al., 2018) or cell transformation into a myofibroblast-like phenotype with filopodia and thus support the ability to migrate into cancer cell nests (Ren et al., 2018). Pancreatic stellate cells (PSCs) create a fibrotic microenvironment and induce hypoxia inside the tumour, ultimately resulting into a hypoxia-fibrosis-cycle. This could be a mechanism to create anaerobic cancer cells, which may be more aggressive (Neuzillet et al., 2014). Furthermore, TGFβ also has immune suppressive functions by inhibiting or activating numerous different immune cells.

In summary, TGFβ is a pro-fibrotic and immunosuppressive agent. Through the induction of desmoplasia and immune cell evasion of pancreatic cancer cells, it creates a favourable context for cancer development and progression.

Histopathological analysis of PKTo mice also showed stromal reaction of pancreatic tissue. Even though no invasive lesions were generated, only few functional acini were observed in very young animals (three months of age). On the other hand, FKTo mice with induction of TGFβ at three months did not display such a rich stromal reaction. Further analysis of the surrounding tumour microenvironment is required to understand the fibrotic reaction in context of premalignant cells.

6.4.2 TGFβ and EMT

Epithelial to mesenchymal transition, at first introduced as “Epithelial to mesenchymal transformation” (Hay, 1995), describes a genetic, cellular process of converting from an epithelial cell type to a mesenchymal type. Afterwards, the name was changed to “transition”, since the process can be also carried out only partially (partial EMT) or

reversed (mesenchymal to epithelial transition, MET). The combination of both EMT and MET is suspected to be essential for metastasis of malignant cells.

EMT is not a pathological occurrence itself and three different types of EMT are defined. EMT type I is associated with embryonic stem cell differentiation, organ development and formation, type II is present in wound healing, tissue regeneration and organ fibrosis as a response to tissue damage, whereas EMT Type III occurs in neoplastic cells (Kalluri & Weinberg, 2009).

The underlying molecular program of these types is very similar, as the genetic hallmarks of EMT like downregulation of E-Cadherin or upregulation of key EMT transcription factors (EMT-TF) like SNAI1, TWIST or ZEB proteins are present in all types of EMT (J. Yang et al., 2020).

Epithelial cells usually form a cell complex and are often located at a basement membrane, communicating through their intercellular junctions. They show an unequal distribution of certain proteins to maintain the integrity of their cell junctions, which is called apical-basal polarity. Undergoing EMT, these cells lose their cell-cell-junctions through dissolution of tight junctions, repression of claudin and occludin, accompanied by the degredation of E-Cadherin on the cell surface, thus reducing cell adhesion (Lamouille, Xu, & Derynck, 2014). At the same time, mesenchymal neural cadherin (N-cadherin) is upregulated. This process is called “cadherin switch”. The cells undergo actin rearrangement, which leads to a switch to front-rear polarity, reduced cell adhesion und ultimately changing the cells shape. The cell is slowly degrading the extracellular matrix (ECM) mostly via matrix metalloproteases to escape its neighbouring cells and gain motility (Lamouille et al., 2014). These three major adaptions (deconstruction of cell junctions, polarity change and cytoskeletal change) enable EMT. Key EMT-TF, leading to above mentioned changes, use various pathways to initiate this process.

TGFβ family proteins are presumed to play a role with all three EMT types and TGFβ uses both, SMAD- and non-SMAD-mediated signalling to affect and progress EMT (Kalluri & Weinberg, 2009). Increased attention for TGFβ compared to other EMT inducers arose, because it is a potent inducer of EMT in cell culture and can therefore be used well for experiments targeting EMT processes (Miettinen, Ebner, Lopez, & Derynck, 1994).

The SMAD complexes can either directly alter protein translation through their DNA-binding ability or indirectly increase the activity of key EMT-TFs. Examples are the repression of E-Cadherin and occludin genes, repression of ID1, hence facilitating TWIST, expression or induction of ZEB1 or SNAI1 expression. Non-SMAD signalling works through interaction with RHO-like GTPases, PI3K or MAPK pathways and several others.

These targets regulate various parts of EMT processes including cell growth, proliferation and motility (Hao, Baker, & Ten Dijke, 2019).

As TGFβ is also known for its tumour suppressive functions, it is still unclear how cancer cells enable the process of TGFβ-induced EMT. On one hand, about 50% of patients with pancreatic cancer show mutations inhibiting TGFβ signal transduction, presumably inhibiting its tumour suppressive role, while leaving tumour promoting factors intact. On the other hand, theories on the remaining 50% of cases diverge in literature. Recent studies proposed an escape mechanism through high ID1 levels, which decouples TGFβ-induced EMT from apoptosis (Huang et al., 2020).

As EMT type III is regarded as a pro-metastatic event, TGFβ-mediated EMT is used as a prime example for tumour promoting effects of TGFβ. Interestingly, a study in 2016 postulated a tumour-suppressive role of this mechanism due to lethal EMT initiated by TGFβ (David et al., 2016).

In summary, induction of EMT through TGFβ is commonly accepted as a facilitator of metastasis in cancer cells and therefore a driver of tumour progression. Crosstalk between TGFβ pathways and known EMT key drivers have been demonstrated, but are still subjects to studies today. A further investigation of mechanisms in our mouse model could result in a better understanding of the distinct trajectories leading to aggressive phenotype and 100 % metastasis rate.

Acknowledgments

I would like to thank everyone who has helped me during the work on this doctoral thesis project.

First, I would like to express my gratitude to my supervisor Prof. Dr. Dieter Saur for giving me the opportunity to work on this project in his lab and his support and supervision over these years.

I especially thank Prof. Dr. Günter Schneider for his scientific input as mentor to this thesis.

Many thanks go to Magda Zukowska, who taught me the methods required for this project, Dr. Moritz Jessinghaus for pathological analysis and the animal caretakers in our mouse facility.
I am also grateful to Tania Custodia Santos, who took over the project and with whom I discussed direction of this project.
I especially thank Stephanie Bärthel for her support and proofreading this thesis.

I thank all members of the Saur, Schneider, Reichert and Rad labs for their great scientific input and the professional work environment.

Finally, I would like to thank my family and friends, especially my parents and my partner Kai Fritzsche – without their constant support and encouragement this thesis would not have been possible.

References

Adamska, A., Domenichini, A., & Falasca, M. (2017). Pancreatic Ductal Adenocarcinoma: Current and Evolving Therapies. *Int J Mol Sci, 18*(7). doi:10.3390/ijms18071338

Almoguera, C., Shibata, D., Forrester, K., Martin, J., Arnheim, N., & Perucho, M. (1988). Most human carcinomas of the exocrine pancreas contain mutant c-K-ras genes. *Cell, 53*(4), 549-554. Retrieved from https://www.ncbi.nlm.nih.gov/pubmed/2453289

Bardeesy, N., Cheng, K. H., Berger, J. H., Chu, G. C., Pahler, J., Olson, P., . . . DePinho, R. A. (2006). Smad4 is dispensable for normal pancreas development yet critical in progression and tumor biology of pancreas cancer. *Genes Dev, 20*(22), 3130-3146. doi:10.1101/gad.1478706

Basturk, O., Hong, S. M., Wood, L. D., Adsay, N. V., Albores-Saavedra, J., Biankin, A. V., . . . Baltimore Consensus, M. (2015). A Revised Classification System and Recommendations From the Baltimore Consensus Meeting for Neoplastic Precursor Lesions in the Pancreas. *Am J Surg Pathol, 39*(12), 1730-1741. doi:10.1097/PAS.0000000000000533

Batlle, E., & Massague, J. (2019). Transforming Growth Factor-beta Signaling in Immunity and Cancer. *Immunity, 50*(4), 924-940. doi:10.1016/j.immuni.2019.03.024

Beato, F., Reveron, D., Dezsi, K. B., Ortiz, A., Johnson, J. O., Chen, D. T., . . . Fleming, J. B. (2021). Establishing a living biobank of patient-derived organoids of intraductal papillary mucinous neoplasms of the pancreas. *Lab Invest, 101*(2), 204-217. doi:10.1038/s41374-020-00494-1

Bos, J. L., Rehmann, H., & Wittinghofer, A. (2007). GEFs and GAPs: critical elements in the control of small G proteins. *Cell, 129*(5), 865-877. doi:10.1016/j.cell.2007.05.018

Brummelkamp, T. R., Bernards, R., & Agami, R. (2002). Stable suppression of tumorigenicity by virus-mediated RNA interference. *Cancer Cell, 2*(3), 243-247. doi:10.1016/s1535-6108(02)00122-8

Collins, M. A., & Pasca di Magliano, M. (2013). Kras as a key oncogene and therapeutic target in pancreatic cancer. *Front Physiol, 4*, 407. doi:10.3389/fphys.2013.00407

Collisson, E. A., Trejo, C. L., Silva, J. M., Gu, S., Korkola, J. E., Heiser, L. M., . . . McMahon, M. (2012). A central role for RAF-->MEK-->ERK signaling in the genesis of pancreatic ductal adenocarcinoma. *Cancer Discov, 2*(8), 685-693. doi:10.1158/2159-8290.CD-11-0347

Conroy, T., Hammel, P., Hebbar, M., Ben Abdelghani, M., Wei, A. C., Raoul, J. L., . . . the Unicancer, G. I. P. G. (2018). FOLFIRINOX or Gemcitabine as Adjuvant Therapy for Pancreatic Cancer. *N Engl J Med, 379*(25), 2395-2406. doi:10.1056/NEJMoa1809775

Constam, D. B. (2014). Regulation of TGFbeta and related signals by precursor processing. *Semin Cell Dev Biol, 32*, 85-97. doi:10.1016/j.semcdb.2014.01.008

Coussens, L. M., & Werb, Z. (2002). Inflammation and cancer. *Nature, 420*(6917), 860-867. doi:10.1038/nature01322

Cox, A. D., Fesik, S. W., Kimmelman, A. C., Luo, J., & Der, C. J. (2014). Drugging the undruggable RAS: Mission possible? *Nat Rev Drug Discov, 13*(11), 828-851. doi:10.1038/nrd4389

Daopin, S., Piez, K. A., Ogawa, Y., & Davies, D. R. (1992). Crystal structure of transforming growth factor-beta 2: an unusual fold for the superfamily. *Science, 257*(5068), 369-373. doi:10.1126/science.1631557

David, C. J., Huang, Y. H., Chen, M., Su, J., Zou, Y., Bardeesy, N., . . . Massague, J. (2016). TGF-beta Tumor Suppression through a Lethal EMT. *Cell, 164*(5), 1015-1030. doi:10.1016/j.cell.2016.01.009

David, C. J., & Massague, J. (2018). Contextual determinants of TGFbeta action in development, immunity and cancer. *Nat Rev Mol Cell Biol, 19*(7), 419-435. doi:10.1038/s41580-018-0007-0

Distler, M., Aust, D., Weitz, J., Pilarsky, C., & Grutzmann, R. (2014). Precursor lesions for sporadic pancreatic cancer: PanIN, IPMN, and MCN. *Biomed Res Int, 2014*, 474905. doi:10.1155/2014/474905

Downward, J. (2004). PI 3-kinase, Akt and cell survival. *Semin Cell Dev Biol, 15*(2), 177-182. doi:10.1016/j.semcdb.2004.01.002

Drosten, M., & Barbacid, M. (2020). Targeting the MAPK Pathway in KRAS-Driven Tumors. *Cancer Cell, 37*(4), 543-550. doi:10.1016/j.ccell.2020.03.013

Duda, D. G., Sunamura, M., Lefter, L. P., Furukawa, T., Yokoyama, T., Yatsuoka, T., . . . Horii, A. (2003). Restoration of SMAD4 by gene therapy reverses the invasive phenotype in pancreatic adenocarcinoma cells. *Oncogene, 22*(44), 6857-6864. doi:10.1038/sj.onc.1206751

Ebisawa, T., Fukuchi, M., Murakami, G., Chiba, T., Tanaka, K., Imamura, T., & Miyazono, K. (2001). Smurf1 interacts with transforming growth factor-beta type I receptor through Smad7 and induces receptor degradation. *J Biol Chem, 276*(16), 12477-12480. doi:10.1074/jbc.C100008200

Eser, S., Reiff, N., Messer, M., Seidler, B., Gottschalk, K., Dobler, M., . . . Saur, D. (2013). Selective requirement of PI3K/PDK1 signaling for Kras oncogene-driven pancreatic cell plasticity and cancer. *Cancer Cell, 23*(3), 406-420. doi:10.1016/j.ccr.2013.01.023

Eser, S., Schnieke, A., Schneider, G., & Saur, D. (2014). Oncogenic KRAS signalling in pancreatic cancer. *Br J Cancer, 111*(5), 817-822. doi:10.1038/bjc.2014.215

Friess, H., Yamanaka, Y., Buchler, M., Ebert, M., Beger, H. G., Gold, L. I., & Korc, M. (1993). Enhanced expression of transforming growth factor beta isoforms in pancreatic cancer correlates with decreased survival. *Gastroenterology, 105*(6), 1846-1856. doi:10.1016/0016-5085(93)91084-u

Goebel, E. J., Hart, K. N., McCoy, J. C., & Thompson, T. B. (2019). Structural biology of the TGFbeta family. *Exp Biol Med (Maywood), 244*(17), 1530-1546. doi:10.1177/1535370219880894

Guerra, C., & Barbacid, M. (2013). Genetically engineered mouse models of pancreatic adenocarcinoma. *Mol Oncol, 7*(2), 232-247. doi:10.1016/j.molonc.2013.02.002

Hao, Y., Baker, D., & Ten Dijke, P. (2019). TGF-beta-Mediated Epithelial-Mesenchymal Transition and Cancer Metastasis. *Int J Mol Sci, 20*(11). doi:10.3390/ijms20112767

Hay, E. D. (1995). An overview of epithelio-mesenchymal transformation. *Acta Anat (Basel), 154*(1), 8-20. doi:10.1159/000147748

Hieber, M. S. (2021). *Molekulare Analyse der Metastasierung des Pankreaskarzinoms.* (Dissertation). Technische Universität München, Retrieved from http://nbn-resolving.de/urn/resolver.pl?urn:nbn:de:bvb:91-diss-20210222-1575209-1-3

Hingorani, S. R., Petricoin, E. F., Maitra, A., Rajapakse, V., King, C., Jacobetz, M. A., . . . Tuveson, D. A. (2003). Preinvasive and invasive ductal pancreatic cancer and its early detection in the mouse. *Cancer Cell, 4*(6), 437-450. Retrieved from https://www.ncbi.nlm.nih.gov/pubmed/14706336

Holm, T. M., Habashi, J. P., Doyle, J. J., Bedja, D., Chen, Y., van Erp, C., . . . Dietz, H. C. (2011). Noncanonical TGFbeta signaling contributes to aortic aneurysm progression in Marfan syndrome mice. *Science, 332*(6027), 358-361. doi:10.1126/science.1192149

Hruban, R. H., Adsay, N. V., Albores-Saavedra, J., Compton, C., Garrett, E. S., Goodman, S. N., . . . Offerhaus, G. J. (2001). Pancreatic intraepithelial neoplasia: a new nomenclature and classification system for pancreatic duct lesions. *Am J Surg Pathol, 25*(5), 579-586. doi:10.1097/00000478-200105000-00003

Hruban, R. H., Maitra, A., & Goggins, M. (2008). Update on pancreatic intraepithelial neoplasia. *Int J Clin Exp Pathol, 1*(4), 306-316. Retrieved from https://www.ncbi.nlm.nih.gov/pubmed/18787611

Huang, Y. H., Hu, J., Chen, F., Lecomte, N., Basnet, H., David, C. J., . . . Massague, J. (2020). ID1 Mediates Escape from TGFbeta Tumor Suppression in Pancreatic Cancer. *Cancer Discov, 10*(1), 142-157. doi:10.1158/2159-8290.CD-19-0529

Ijichi, H., Chytil, A., Gorska, A. E., Aakre, M. E., Fujitani, Y., Fujitani, S., . . . Moses, H. L. (2006). Aggressive pancreatic ductal adenocarcinoma in mice caused by pancreas-specific blockade of transforming growth factor-beta signaling in cooperation with active Kras expression. *Genes Dev, 20*(22), 3147-3160. doi:10.1101/gad.1475506

Izeradjene, K., Combs, C., Best, M., Gopinathan, A., Wagner, A., Grady, W. M., . . . Hingorani, S. R. (2007). Kras(G12D) and Smad4/Dpc4 haploinsufficiency cooperate to induce mucinous cystic neoplasms and invasive adenocarcinoma of the pancreas. *Cancer Cell, 11*(3), 229-243. doi:10.1016/j.ccr.2007.01.017

Jackson, E. L., Willis, N., Mercer, K., Bronson, R. T., Crowley, D., Montoya, R., . . . Tuveson, D. A. (2001). Analysis of lung tumor initiation and progression using conditional expression of oncogenic K-ras. *Genes Dev, 15*(24), 3243-3248. doi:10.1101/gad.943001

Jakowlew, S. B. (2006). Transforming growth factor-beta in cancer and metastasis. *Cancer Metastasis Rev, 25*(3), 435-457. doi:10.1007/s10555-006-9006-2

Jones, S., Zhang, X., Parsons, D. W., Lin, J. C., Leary, R. J., Angenendt, P., . . . Kinzler, K. W. (2008). Core signaling pathways in human pancreatic cancers revealed by global genomic analyses. *Science, 321*(5897), 1801-1806. doi:10.1126/science.1164368

Kalluri, R., & Weinberg, R. A. (2009). The basics of epithelial-mesenchymal transition. *J Clin Invest, 119*(6), 1420-1428. doi:10.1172/JCI39104

Kanda, M., Matthaei, H., Wu, J., Hong, S. M., Yu, J., Borges, M., . . . Goggins, M. (2012). Presence of somatic mutations in most early-stage pancreatic intraepithelial neoplasia. *Gastroenterology, 142*(4), 730-733 e739. doi:10.1053/j.gastro.2011.12.042

Kawaguchi, Y., Cooper, B., Gannon, M., Ray, M., MacDonald, R. J., & Wright, C. V. (2002). The role of the transcriptional regulator Ptf1a in converting intestinal to pancreatic progenitors. *Nat Genet, 32*(1), 128-134. doi:10.1038/ng959

Kojima, K., Vickers, S. M., Adsay, N. V., Jhala, N. C., Kim, H. G., Schoeb, T. R., . . . Klug, C. A. (2007). Inactivation of Smad4 accelerates Kras(G12D)-mediated pancreatic neoplasia. *Cancer Res, 67*(17), 8121-8130. doi:10.1158/0008-5472.CAN-06-4167

Korkut, A., Zaidi, S., Kanchi, R. S., Rao, S., Gough, N. R., Schultz, A., . . . Akbani, R. (2018). A Pan-Cancer Analysis Reveals High-Frequency Genetic Alterations in Mediators of Signaling by the TGF-beta Superfamily. *Cell Syst, 7*(4), 422-437 e427. doi:10.1016/j.cels.2018.08.010

Kramer, E. L., & Clancy, J. P. (2018). TGFbeta as a therapeutic target in cystic fibrosis. *Expert Opin Ther Targets, 22*(2), 177-189. doi:10.1080/14728222.2018.1406922

Lamouille, S., & Derynck, R. (2007). Cell size and invasion in TGF-beta-induced epithelial to mesenchymal transition is regulated by activation of the mTOR pathway. *J Cell Biol, 178*(3), 437-451. doi:10.1083/jcb.200611146

Lamouille, S., Xu, J., & Derynck, R. (2014). Molecular mechanisms of epithelial-mesenchymal transition. *Nat Rev Mol Cell Biol, 15*(3), 178-196. doi:10.1038/nrm3758

Larisch, S., Yi, Y., Lotan, R., Kerner, H., Eimerl, S., Tony Parks, W., . . . Roberts, A. B. (2000). A novel mitochondrial septin-like protein, ARTS, mediates apoptosis dependent on its P-loop motif. *Nat Cell Biol, 2*(12), 915-921. doi:10.1038/35046566

Lawler, S., Feng, X. H., Chen, R. H., Maruoka, E. M., Turck, C. W., Griswold-Prenner, I., & Derynck, R. (1997). The type II transforming growth factor-beta receptor autophosphorylates not only on serine and threonine but also on tyrosine residues. *J Biol Chem, 272*(23), 14850-14859. doi:10.1074/jbc.272.23.14850

Lim, K. H., Baines, A. T., Fiordalisi, J. J., Shipitsin, M., Feig, L. A., Cox, A. D., . . . Counter, C. M. (2005). Activation of RalA is critical for Ras-induced tumorigenesis of human cells. *Cancer Cell, 7*(6), 533-545. doi:10.1016/j.ccr.2005.04.030

Lohr, M., Kloppel, G., Maisonneuve, P., Lowenfels, A. B., & Luttges, J. (2005). Frequency of K-ras mutations in pancreatic intraductal neoplasias associated with pancreatic ductal adenocarcinoma and chronic pancreatitis: a meta-analysis. *Neoplasia, 7*(1), 17-23. doi:10.1593/neo.04445

Lohr, M., Schmidt, C., Ringel, J., Kluth, M., Muller, P., Nizze, H., & Jesnowski, R. (2001). Transforming growth factor-beta1 induces desmoplasia in an experimental model of human pancreatic carcinoma. *Cancer Res, 61*(2), 550-555. Retrieved from https://www.ncbi.nlm.nih.gov/pubmed/11212248

Luo, K. (2017). Signaling Cross Talk between TGF-beta/Smad and Other Signaling Pathways. *Cold Spring Harb Perspect Biol, 9*(1). doi:10.1101/cshperspect.a022137

Malumbres, M., & Barbacid, M. (2003). RAS oncogenes: the first 30 years. *Nat Rev Cancer, 3*(6), 459-465. doi:10.1038/nrc1097

Massague, J. (2008). TGFbeta in Cancer. *Cell, 134*(2), 215-230. doi:10.1016/j.cell.2008.07.001

Massague, J. (2012). TGFbeta signalling in context. *Nat Rev Mol Cell Biol, 13*(10), 616-630. doi:10.1038/nrm3434

Matthaei, H., Schulick, R. D., Hruban, R. H., & Maitra, A. (2011). Cystic precursors to invasive pancreatic cancer. *Nat Rev Gastroenterol Hepatol, 8*(3), 141-150. doi:10.1038/nrgastro.2011.2

Miettinen, P. J., Ebner, R., Lopez, A. R., & Derynck, R. (1994). TGF-beta induced transdifferentiation of mammary epithelial cells to mesenchymal cells: involvement of type I receptors. *J Cell Biol, 127*(6 Pt 2), 2021-2036. doi:10.1083/jcb.127.6.2021

Mu, Y., Gudey, S. K., & Landstrom, M. (2012). Non-Smad signaling pathways. *Cell Tissue Res, 347*(1), 11-20. doi:10.1007/s00441-011-1201-y

Mueller, S., Engleitner, T., Maresch, R., Zukowska, M., Lange, S., Kaltenbacher, T., . . . Rad, R. (2018). Evolutionary routes and KRAS dosage define pancreatic cancer phenotypes. *Nature, 554*(7690), 62-68. doi:10.1038/nature25459

Mulder, K. M., & Morris, S. L. (1992). Activation of p21ras by transforming growth factor beta in epithelial cells. *J Biol Chem, 267*(8), 5029-5031. Retrieved from https://www.ncbi.nlm.nih.gov/pubmed/1544886

Murakami, T., Hiroshima, Y., Matsuyama, R., Homma, Y., Hoffman, R. M., & Endo, I. (2019). Role of the tumor microenvironment in pancreatic cancer. *Ann Gastroenterol Surg, 3*(2), 130-137. doi:10.1002/ags3.12225

Nakhai, H., Sel, S., Favor, J., Mendoza-Torres, L., Paulsen, F., Duncker, G. I., & Schmid, R. M. (2007). Ptf1a is essential for the differentiation of GABAergic and glycinergic amacrine cells and horizontal cells in the mouse retina. *Development, 134*(6), 1151-1160. doi:10.1242/dev.02781

Neuzillet, C., de Gramont, A., Tijeras-Raballand, A., de Mestier, L., Cros, J., Faivre, S., & Raymond, E. (2014). Perspectives of TGF-beta inhibition in pancreatic and hepatocellular carcinomas. *Oncotarget, 5*(1), 78-94. doi:10.18632/oncotarget.1569

Notta, F., Chan-Seng-Yue, M., Lemire, M., Li, Y., Wilson, G. W., Connor, A. A., . . . Gallinger, S. (2016). A renewed model of pancreatic cancer evolution based on genomic rearrangement patterns. *Nature, 538*(7625), 378-382. doi:10.1038/nature19823

Okusaka, T., Nakamura, M., Yoshida, M., Kitano, M., Uesaka, K., Ito, Y., . . . Committee for Revision of Clinical Guidelines for Pancreatic Cancer of the Japan Pancreas, S. (2020). Clinical Practice Guidelines for Pancreatic Cancer 2019 From the Japan Pancreas Society: A Synopsis. *Pancreas, 49*(3), 326-335. doi:10.1097/MPA.0000000000001513

Padua, D., & Massague, J. (2009). Roles of TGFbeta in metastasis. *Cell Res, 19*(1), 89-102. doi:10.1038/cr.2008.316

Papageorgis, P. (2015). TGFbeta Signaling in Tumor Initiation, Epithelial-to-Mesenchymal Transition, and Metastasis. *J Oncol, 2015*, 587193. doi:10.1155/2015/587193

Picon, A., Gold, L. I., Wang, J., Cohen, A., & Friedman, E. (1998). A subset of metastatic human colon cancers expresses elevated levels of transforming growth factor beta1. *Cancer Epidemiol Biomarkers Prev, 7*(6), 497-504. Retrieved from https://www.ncbi.nlm.nih.gov/pubmed/9641494

Rahib, L., Smith, B. D., Aizenberg, R., Rosenzweig, A. B., Fleshman, J. M., & Matrisian, L. M. (2014). Projecting cancer incidence and deaths to 2030: the unexpected burden of thyroid, liver, and pancreas cancers in the United States. *Cancer Res, 74*(11), 2913-2921. doi:10.1158/0008-5472.CAN-14-0155

Ren, B., Cui, M., Yang, G., Wang, H., Feng, M., You, L., & Zhao, Y. (2018). Tumor microenvironment participates in metastasis of pancreatic cancer. *Mol Cancer, 17*(1), 108. doi:10.1186/s12943-018-0858-1

Revathidevi, S., & Munirajan, A. K. (2019). Akt in cancer: Mediator and more. *Semin Cancer Biol, 59*, 80-91. doi:10.1016/j.semcancer.2019.06.002

Rifkin, D. B. (2005). Latent transforming growth factor-beta (TGF-beta) binding proteins: orchestrators of TGF-beta availability. *J Biol Chem, 280*(9), 7409-7412. doi:10.1074/jbc.R400029200

Ritchie, M. R. a. H. (2015). „Cancer“. Published online at OurWorldInData.org.

Ryan, D. P., Hong, T. S., & Bardeesy, N. (2014). Pancreatic adenocarcinoma. *N Engl J Med, 371*(22), 2140-2141. doi:10.1056/NEJMc1412266

Saito, H., Tsujitani, S., Oka, S., Kondo, A., Ikeguchi, M., Maeta, M., & Kaibara, N. (2000). An elevated serum level of transforming growth factor-beta 1 (TGF-beta 1) significantly correlated with lymph node metastasis and poor prognosis in patients with gastric carcinoma. *Anticancer Res, 20*(6B), 4489-4493. Retrieved from https://www.ncbi.nlm.nih.gov/pubmed/11205293

Schlunegger, M. P., & Grutter, M. G. (1992). An unusual feature revealed by the crystal structure at 2.2 A resolution of human transforming growth factor-beta 2. *Nature, 358*(6385), 430-434. doi:10.1038/358430a0

Schmierer, B., & Hill, C. S. (2007). TGFbeta-SMAD signal transduction: molecular specificity and functional flexibility. *Nat Rev Mol Cell Biol, 8*(12), 970-982. doi:10.1038/nrm2297

Schneider, G., Schmidt-Supprian, M., Rad, R., & Saur, D. (2017). Tissue-specific tumorigenesis: context matters. *Nat Rev Cancer, 17*(4), 239-253. doi:10.1038/nrc.2017.5

Schonhuber, N., Seidler, B., Schuck, K., Veltkamp, C., Schachtler, C., Zukowska, M., . . . Saur, D. (2014). A next-generation dual-recombinase system for time- and host-specific targeting of pancreatic cancer. *Nat Med, 20*(11), 1340-1347. doi:10.1038/nm.3646

Schönhuber, N., Seidler, B., Schuck, K., Veltkamp, C., Schachtler, C., Zukowska, M., . . . Saur, D. (2014). A next-generation dual-recombinase system for time- and host-specific targeting of pancreatic cancer. *Nat Med*. Retrieved from http://www.ncbi.nlm.nih.gov/entrez/query.fcgi?cmd=Retrieve&db=PubMed&dopt=Citation&list_uids=25326799

Seidler, B., Schmidt, A., Mayr, U., Nakhai, H., Schmid, R. M., Schneider, G., & Saur, D. (2008). A Cre-loxP-based mouse model for conditional somatic gene expression and knockdown in vivo by using avian retroviral vectors. *Proc Natl Acad Sci U S A, 105*(29), 10137-10142. doi:10.1073/pnas.0800487105

Siegel, R. L., Miller, K. D., Fuchs, H. E., & Jemal, A. (2022). Cancer statistics, 2022. *CA Cancer J Clin, 72*(1), 7-33. doi:10.3322/caac.21708

Simanshu, D. K., Nissley, D. V., & McCormick, F. (2017). RAS Proteins and Their Regulators in Human Disease. *Cell, 170*(1), 17-33. doi:10.1016/j.cell.2017.06.009

Simeone, D. M., Zhang, L., Graziano, K., Nicke, B., Pham, T., Schaefer, C., & Logsdon, C. D. (2001). Smad4 mediates activation of mitogen-activated protein kinases by TGF-beta in pancreatic acinar cells. *Am J Physiol Cell Physiol, 281*(1), C311-319. doi:10.1152/ajpcell.2001.281.1.C311

Siveke, J. T., Einwachter, H., Sipos, B., Lubeseder-Martellato, C., Kloppel, G., & Schmid, R. M. (2007). Concomitant pancreatic activation of Kras(G12D) and Tgfa results in cystic papillary neoplasms reminiscent of human IPMN. *Cancer Cell, 12*(3), 266-279. doi:10.1016/j.ccr.2007.08.002

Smit, V. T., Boot, A. J., Smits, A. M., Fleuren, G. J., Cornelisse, C. J., & Bos, J. L. (1988). KRAS codon 12 mutations occur very frequently in pancreatic adenocarcinomas. *Nucleic Acids Res, 16*(16), 7773-7782. doi:10.1093/nar/16.16.7773

Strickler, J. H., Satake, H., Hollebecque, A., Sunakawa, Y., Tomasini, P., Bajor, D. L., . . . Hong, D. S. (2022). First data for sotorasib in patients with pancreatic cancer with KRAS p.G12C mutation: A phase I/II study evaluating efficacy and safety. *Journal of Clinical Oncology, 40*(36_suppl), 360490-360490. doi:10.1200/JCO.2022.40.36_suppl.360490

Sun, Q., Zhang, B., Hu, Q., Qin, Y., Xu, W., Liu, W., . . . Xu, J. (2018). The impact of cancer-associated fibroblasts on major hallmarks of pancreatic cancer. *Theranostics, 8*(18), 5072-5087. doi:10.7150/thno.26546

Syed, V. (2016). TGF-beta Signaling in Cancer. *J Cell Biochem, 117*(6), 1279-1287. doi:10.1002/jcb.25496

Theodosiou, N. A., & Xu, T. (1998). Use of FLP/FRT system to study Drosophila development. *Methods, 14*(4), 355-365. doi:10.1006/meth.1998.0591

Tucker, R. F., Shipley, G. D., Moses, H. L., & Holley, R. W. (1984). Growth inhibitor from BSC-1 cells closely related to platelet type beta transforming growth factor. *Science, 226*(4675), 705-707. doi:10.1126/science.6093254

Turco, A., Coppa, A., Aloe, S., Baccheschi, G., Morrone, S., Zupi, G., & Colletta, G. (1999). Overexpression of transforming growth factor beta-type II receptor reduces tumorigenicity and metastastic potential of K-ras-transformed thyroid cells. *Int J Cancer, 80*(1), 85-91. doi:10.1002/(sici)1097-0215(19990105)80:1<85::aid-ijc17>3.0.co;2-p

Tyler Stevens, M. L. C., MD, MS. (2020). Exocrine pancreatic insufficiency. Retrieved from https://www.uptodate.com/contents/exocrine-pancreatic-insufficiency?search=pancreas%20insufficiency&source=search_result&selectedTitle=1~117&usage_type=default&display_rank=1

Vogelstein, B., Fearon, E. R., Hamilton, S. R., Kern, S. E., Preisinger, A. C., Leppert, M., . . . Bos, J. L. (1988). Genetic alterations during colorectal-tumor development. *N Engl J Med, 319*(9), 525-532. doi:10.1056/NEJM198809013190901

Wagner, M., Kleeff, J., Friess, H., Buchler, M. W., & Korc, M. (1999). Enhanced expression of the type II transforming growth factor-beta receptor is associated with decreased survival in human pancreatic cancer. *Pancreas, 19*(4), 370-376. doi:10.1097/00006676-199911000-00008

Wang, J., Sun, L., Myeroff, L., Wang, X., Gentry, L. E., Yang, J., . . . et al. (1995). Demonstration that mutation of the type II transforming growth factor beta receptor inactivates its tumor suppressor activity in replication error-positive colon carcinoma cells. *J Biol Chem, 270*(37), 22044-22049. doi:10.1074/jbc.270.37.22044

Yang, G., & Yang, X. (2010). Smad4-mediated TGF-beta signaling in tumorigenesis. *Int J Biol Sci, 6*(1), 1-8.

Yang, J., Antin, P., Berx, G., Blanpain, C., Brabletz, T., Bronner, M., . . . Association, E. M. T. I. (2020). Guidelines and definitions for research on epithelial-mesenchymal transition. *Nat Rev Mol Cell Biol, 21*(6), 341-352. doi:10.1038/s41580-020-0237-9

Yao, N., Coryell, L., Zhang, D., Georgescu, R. E., Finkelstein, J., Coman, M. M., . . . O'Donnell, M. (2003). Replication factor C clamp loader subunit arrangement within the circular pentamer and its attachment points to proliferating cell nuclear antigen. *J Biol Chem, 278*(50), 50744-50753. doi:10.1074/jbc.M309206200

Zhang, Y. E. (2009). Non-Smad pathways in TGF-beta signaling. *Cell Res, 19*(1), 128-139. doi:10.1038/cr.2008.328

Zhang, Y. E. (2017). Non-Smad Signaling Pathways of the TGF-beta Family. *Cold Spring Harb Perspect Biol, 9*(2). doi:10.1101/cshperspect.a022129